

1 Response to Referee 1 Comments on “The G4Foam Experiment: Global Impacts of Regional
2 Ocean Albedo Modification,” by C. J. Gabriel et al.

3
4 Referee comments are in black. Responses are in blue.

5
6 1) In the case of termination of G4Foam, why not study a gradual termination instead of an
7 abrupt termination? It would be interesting to see the recovering phase of G4Foam in a gradual
8 termination process.

9
10 It would be interesting to study a slower return to reference simulation conditions
11 probably not only in G4Foam, but in other GeoMIP experiments as well. However, all GeoMIP
12 experiments to date that have included termination, including G4SSA, have imposed abrupt
13 termination. We keep to this convention to facilitate comparison with RCP6.0 and G4SSA. If
14 one has simulated a large step response, it is straightforward to scale the results to a more gradual
15 response. The abrupt change has the advantage of a large signal-to-noise ratio, so the response is
16 easily identified.

17
18 2) Paper claims the G4Foam experiment would cool the NH tropics and hence reduce the heat
19 related mortality (Line no : 127, 377). However, heat related mortality is caused by extreme
20 temperatures not the mean values, please justify.

21
22 We have eliminated the assertion that G4Foam would reduce heat-related mortality, as
23 we have found that this may not be true. The following text has been added to the manuscript.
24 Please see lines 100-115 in the revised manuscript.

25
26 “The asymmetric cooling would force changes in the Hadley Cell, enhancing cross-
27 equatorial flow, which would cool the surface in the NH tropics, especially during JJA, when
28 heat mortality and morbidity is highest. However, despite a reduction in the JJA mean
29 temperature in the tropics, extreme events are responsible for most heat-related mortality and
30 morbidity, and the reduction in the mean temperature does not necessarily mean that there will
31 be a reduction in the type of extreme heat events that cause human tragedy. While Kharin et al.
32 (2007) showed that, in general, temperature extremes track with the mean temperature, this is not
33 always the case. The changes in extreme events may, for example, be greater at high latitudes
34 and the variability of temperatures over land may increase in a warmer climate.

35 “Specific to geoengineering, Aswathy et al. (2015) showed that different climate
36 engineering methods produce spatially heterogeneous changes in extreme precipitation and
37 temperature events. They showed that one SRM scheme may be more effective than another in
38 reducing different types of extreme events despite relatively similar global and regional mean
39 responses. In particular, a marine cloud brightening scheme that brightens ocean areas between
40 30°N and 30°S is shown to be less effective in reducing extreme precipitation and temperature
41 events over land than the G3 experiment is.”

42
43 Aswathy et al. (2015) used output from three different earth system models, each with
44 multiple ensemble members, and performed detailed analysis of five variables related to extreme
45 events. In the event more modeling groups run G4Foam, or we run other similar test bed
46 experiments, that type of analysis would be valuable. Our goal in this testbed experiment is to
47 describe the G4Foam experiment and describe some of the mechanisms that bring about the
48 mean climate response.

49
50
51
52
53
54
55
56
57
58
59
60
61
62
63
64
65
66
67
68
69
70
71
72
73
74
75
76
77
78
79
80
81
82
83
84
85
86
87
88
89
90
91
92
93
94
95
96

3) Line no 382-386 : Please provide the values in comparison with RCP6.0?

We now also provide the values relative to RCP6.0.

4) From Table1 (also from Figure 6) it is clear that the G4Foam experiment increases the tropical land precipitation by 1.4% annually and 2.02% during JJA relative to RCP6.0. How does this affect the extreme precipitation and frequent flooding events occurring in tropical land regions during monsoon time? Similar to reduction in precipitation, excess precipitation also affects the society right? So does this cause more adverse affects than benefits?

This is an important point and we have removed references to the desirability or benefits of any of the respective hydrological regimes under G4SSA, G4Foam and RCP6.0 in the manuscript. G4Foam was designed to cool Earth and increase precipitation, particularly in the tropics, relative to G4SSA. The fact that G4Foam produces this excess precipitation response relative to RCP6.0 is one of the reasons why we mention in 4.4 Future Research that we may combine stratospheric SRM with surface albedo modification to more effectively cool the planet without increasing precipitation to a level above that under RCP6.0 in already wet tropical areas. The manuscript has been adjusted. We are endeavoring to portray a balanced picture of the climate effects of G4Foam. We remain agnostic as to whether those climate effects are good or bad. In particular, section 3.2 Hydrological Impacts now offers a balanced description of the results of G4Foam, as does 4.3 Caveats. Future work that considers extreme events and natural resource economics may address whether the climate impacts brought about G4Foam ultimately can be rigorously characterized as more adverse or more beneficial both regionally and globally.

5) Line no : 461-463, (Similar to the above point) How can it be an important benefit without analyzing the effects of increased precipitation especially during monsoon season. Extreme precipitation may lead to more floods adversely affecting the societies. Could you please justify this point with further analysis.

We now emphasize that a precipitation increase in G4Foam relative to RCP6.0 is not the goal of G4Foam. We have also withdrawn the claims about beneficial changes in water supply and instead only discuss changes in P-E. More broadly, we have removed normative language about “benefits” and desirability” of the precipitation response, and instead just report the scientific results. This manuscript is designed to describe the results of the experiment and to describe the mean response and describe the relevant mechanisms. To justify our points about G4Foam being beneficial to water supply, it would be necessary to study both extreme events and the economic, policy and resource allocation factors that determine the availability of water in a particular area.

6) Line no : 472-474 Could you please give more explanation to the hypothesis.

Lines 472-474 have been removed. This was an oversimplification with little physical meaning. The key here is the northward migration of the ITCZ and the global scale changes in the Hadley Cell.

7) Discussion part seems to be extremely positive about the precipitation response of G4Foam. Increase in precipitation does not always mean without negative impacts. Please rephrase the

97 discussion with inclusion of the negative impacts of excess water supply and precipitation.

98
99 _____ We have revised the manuscript to portray a more balanced picture of the climate effects
100 of G4Foam. We remain agnostic as to whether those effects are good or bad. Specifically, we
101 have added discussion to section 3.2 Hydrological Response to give more weight to both the
102 negative effects of excessive rainfall in the tropics and the potential for adverse impacts due to
103 reduced rainfall in the SH. Section 4.3 Caveats also discusses potential problems with G4Foam.
104 Finally, the paper ends with section 4.4 Future Work. While the climate response in G4Foam is
105 robust in that it cools important regions and changes the spatial distribution of rainfall in a way
106 that may be favorable for some, G4Foam has obvious deficiencies. For example, NH land areas
107 are not cooled very much, precipitation increases too much in already wet tropical regions, and
108 parts of the SH receive a very large decrease in precipitation. Additionally, since we do not aim
109 to describe changes in the distribution of extreme events, we eliminate discussion of “water
110 supply” and instead discuss precipitation minus evaporation. A higher or lower amount of
111 extreme precipitation events could increase or decrease runoff, which would then impact water
112 supply independent of precipitation minus evaporation.

113 Technical corrections

114 Line no : 91 Please provide expansion of SSI.

115 _____
116 Stratospheric sulfate injection (SSI) is now defined.

117 _____
118 Line no : 188 Could you please rephrase the sentence for better understanding.

119 _____
120 You are correct to point out that this sentence was confusing. The purpose here was to
121 describe the mechanism underlying the southward migration of the ITCZ. We have clarified the
122 sentence, which now reads “The forced cooling over the NH was enhanced by a positive
123 dynamical feedback in the North Atlantic Ocean (Broccoli et al. 2006; Kang et al. 2008), and the
124 ITCZ and associated tropical rainbelts migrated south.” There is no need to bring up the energy-
125 flux-equator here.

126 _____
127 Line no : 335 This is for JJA season right? please specify it.

128 _____
129 Yes. During JJA added.

130 _____
131 Line no : 343 Is it G4Foam or G4SSA?

132 _____
133 We meant G4SSA and have changed G4Foam to G4SSA in that sentence.

134 _____
135 Line no : 396 Please check the value with the one given in Table1.

136 _____
137 The values in the table were correct. We changed the text to reflect those values.

138 _____
139 Line no : 398 Shouldn't it be RCP6.0 instead of G4SSA?

140 _____
141 Yes. We changed it to RCP6.0

145 Line no : 406 Please check the values with Table1, values seems to be interchanged.

146

147 We checked the values and there were a couple mistakes in the text. We fixed those
148 mistakes and the values in the text now match the values in Table 1.

149

150 Line no : 856 Typo in Figure caption.

151

152 Typo fixed.

153

154 We have also shortened the abstract by one sentence. Line 646-647 added to acknowledgements
155 to thank you for your valuable comments.

156

157

158

References

159

160 Aswathy, V. N., Boucher, O., Quaas, M., Niemeier, U., Muri, H., Mülmenstädt, J., and Quaas, J.:
161 Climate extremes in multi-model simulations of stratospheric aerosol and marine cloud
162 brightening climate engineering, Atmos. Chem. Phys., 15, 9593-9610, doi:10.5194/acp-15-
163 9593-2015, 2015.

164

165 Kharin, V. V., Zwiers, F. W., Zhang, X., and Hegerl, G. C.: Changes in temperature and
166 precipitation extremes in the IPCC ensemble of Global Coupled Model Simulations, J.
167 Climate, 20, 1419– 1444, doi:10.1175/JCLI4066.1, 2007.

168

169

170 Response to Referee 2 Comments on “The G4Foam Experiment: Global Impacts of Regional
171 Ocean Albedo Modification,” by C. J. Gabriel et al.

172
173 Referee comments are in black. Responses are in blue.

174
175 1) The introduction session is a bit too long. Some of the background information for
176 geoengineering in general, motivation and review can be shortened.

177
178 _____ We agree and have removed the excess background information on geoengineering,
179 reduced the length of the motivation section and the amount of literature review. Please see the
180 new, ~35% shorter, introduction section. We were also able to remove some redundant language
181 in sections 2-4 to make the paper a bit shorter.

182 Discussion paper

183 2) In many of the figures results are shown and discussed in terms of both annual mean and June-
184 July-August (JJA) seasonal mean. It is unclear why JJA, which is neither austral summer nor the
185 exact monsoon season in the northern hemisphere, is discussed in particular, as opposed to other
186 seasons.

187
188 _____ JJA is chosen because it is meteorological summer in the NH and using JJA facilitates
189 comparison with G4SSA, which reports results in terms of JJA (Xia et al., 2016). However, the
190 Indian Monsoon season is typically defined JJAS, and we would use JJAS as our summer/wet
191 monsoon season if we were focusing primarily on the Indian monsoon, or even exclusively on
192 the Asian monsoon more broadly. Not all precipitation that is of interest in this study is monsoon
193 precipitation, and various monsoon regions do experience somewhat different wet monsoon
194 seasons. The cloud and temperature responses that are most of interest to highly cultivated and
195 populated regions are best expressed by using JJA, since the NH is at its warmest during that
196 meteorological season. Future work associated with the G4SSA and G4Foam simulation may
197 look at, among other things, possible changes in monsoon onset and withdrawal in various
198 geoengineering scenarios relative to what will happen under the RCP scenarios.

199 _____ We add a summary of this reasoning to the text at lines 286-288 of the revised
200 manuscript.

201
202 3) The color scheme in Figures 6-8 is different from that in Figures 3-5. This is fine, but using
203 warm colors for decreases (i.e., negative changes) and cold colors for increases is a little
204 inconvenient. Is there a particular reason for this?

205
206 _____ Yes. The green is intended to signify a wet anomaly, and the brown is used to signify a
207 dry anomaly. This color scheme is only used for hydrological variables precipitation,
208 evaporation and precipitation minus evaporation (P-E). The colors we used are the traditional
209 ones used for those variables, for example in the IPCC reports and in NOAA’s Palmer Drought
210 Index maps.

211
212 4) Line 76 (also in the caption of Figure 1): the phrases of “daily average” and “fixed daytime
213 value” are inconsistent and a little confusing. My understanding is that the albedo is changed
214 from one constant value to another. Is that right?

215
216 _____ The albedo is actually changed from a value with a very small daily cycle that has a daily
217 average value of 0.06 to a constant value of 0.15 (with no daily cycle) in the “foamed” regions.

218 The inconsistent language has been removed. Please see that section, now at lines 50-55 and line
219 57-65, as well as the caption to Figure 1, which more clearly explains the change in albedo we
220 imposed in the model. We have also added the caveat that an actual foamed region would likely
221 exhibit fluctuations in albedo for many reasons and that additional study of the foam itself would
222 be necessary to provide sufficient information to include fluctuations in foamed region albedo in
223 future modeling studies. This could result in a slightly different surface energy budget than the
224 constant albedo foam modeled here.

225
226 “RCP6.0 and G4SSA are run with an ocean surface albedo that contains a very small daily cycle,
227 but the average albedo over a day is 0.06. The albedo of the ocean surface is raised from this
228 daily mean of 0.06 to a constant value of 0.15, with no daily cycle, over the subtropical ocean
229 gyres in the Southern Hemisphere, specifically 20°N-20°S, 90°W-170°W (South Pacific), 20°N-
230 20°S, 30°W-0°E (South Atlantic) and 20°N-20°S, 55°E-105°E (South Indian) (Fig. 1).
231 Everywhere else, ocean surface albedo in G4Foam is calculated the same as in RCP6.0 and
232 G4SSA.”

233
234 5) Lines 88-99: please clarify the use of acronym SSI (versus SAI).

235
236 _____ This was an error in editing. We now define stratospheric sulfate injections as SSI in the
237 revised manuscript and SSI is used exclusively throughout to refer to stratospheric SRM. There
238 is no mention of “SAI” any longer.

239
240 6) Lines 134: “the cloud feedbacks” are unclear.

241
242 _____ We have changed “the cloud feedbacks” to “any cloud feedbacks.” We are
243 acknowledging that the effectiveness of the G4Foam forcing will be affected by how clouds
244 respond to the forcing, that the nature of this response is unknown until we conduct the
245 experiment, and that we consider clouds to potentially be a large source of uncertainty. Please
246 see lines 122-125.

247
248 7) Lines 248-249: Is this likelihood larger in this area than other areas in the SH?
249 Please explain.

250
251 _____ You are correct to point this out. The likelihood is not necessarily larger and the
252 reference to that likelihood has been removed. We were principally motivated to brighten those
253 specific regions because of their low cloud fraction, low wind speeds, weak currents, and lack of
254 biological productivity.

255
256 8) Lines 267-268: Is there a reference for the attribution of model improvements to finite-volume
257 dynamical core?

258
259 _____ Yes. The reference to Neale et al. (2013) has been added at line 228.

260
261 9) Lines 310-311: is there a problem in the phrase inside the double quotes?

262
263 _____ No. We have removed the quotes.

264
265 10) Line 339: needs some hyphens for “clear sky top of atmosphere”

266
267 Hyphens added.

268
269 11) Lines 341-346: it makes more sense to show net all-sky TOA flux in Fig. 2, maybe along
270 with the net cloud forcing. The clear-sky forcing is not what is really exerted to the climate
271 system.

272
273 We agree and have added the new Figure 2, which shows net all-sky TOA flux (Figure
274 2a) and net cloud forcing (Figure 2b). The beginning of section 3.1, now at lines 290-305, now
275 refers to the new Figure 2. Additionally, we now report changes in radiative forcing as the all-
276 sky values, rather than the clear-sky values, since all-sky is what is actually exerted on the
277 climate. Figure 3, showing clear-sky forcing, which is very similar to, and at the beginning of
278 the simulation, is almost exactly equal to, the imposed ocean surface albedo forcing. Clear-sky
279 SW TOA is now only shown to illustrate that the G4Foam forcing is more efficient in achieving
280 cooling than G4SSA forcing.

281
282 12) Lines 366-373: need more evidence to support the explanation for the increase in low-cloud
283 fraction over the three areas, where the relative humidity might have been already quite high.
284 Why doesn't the increase occur in the entire downwind area?

285
286 We have revised the manuscript to provide a detailed explanation for the increase in low
287 cloud fraction in the areas to the north and northeast of the three "foamed" regions. The new
288 section is copied below and can be found at lines 329-373:

289
290 "The low cloud fraction increase in the three areas to the north and northeast of the
291 G4Foam-forced subtropical surface regions is likely due to a stronger than normal trade wind
292 inversion (TWI). The inversion develops when warm air is trapped above the atmospheric
293 mixed layer due to large-scale subsidence and surface mixing of cooler air above these relatively
294 low SST regions. The increase in low cloud fraction does not occur over the entire downwind
295 area because SSTs increase from east to west, causing a change in the lower troposphere as you
296 travel from east to west. Moving west, the stratocumulus layer, which is trapped under the
297 inversion base, decouples from the mixed layer in the lower troposphere. The surface warming
298 triggers more turbulence within the planetary boundary layer, which allows for enhanced
299 cumulus mixing in the cloud layer, which entrains dry air, and the marine stratocumulus layer
300 evaporates as you travel west.

301 "The subtropical high-pressure systems are stronger in G4Foam, due to the stronger than
302 normal Hadley Cell, which enhances subsidence throughout the subtropics. Typically, a
303 subsidence inversion is strongest over the center of the subtropical anticyclones, over cold
304 currents (particularly the Peru Current), and over cooler than normal waters, which are subjected
305 to enhanced upwelling in large part by trade winds on the periphery of the subtropical highs
306 (DeSzoeko et al., 2016). The TWI becomes weaker and its base increases in height with distance
307 towards the west and towards the equator as SSTs increase. This pattern is particularly evident
308 in the Pacific, due to the larger geographical extent of the forced area.

309 "Specifically, under G4Foam conditions, the increased low cloud fraction areas are the
310 result of the combination of enhanced large-scale subsidence (stronger Hadley cell) and a cooler
311 than normal ocean surface. The cooler than normal surface waters are due to general cooling
312 throughout the SH, as well as an increase in wind-driven upwelling over these areas of increased

313 low cloud fraction, which are already prone to upwelling, large fraction of low clouds and high
314 relative humidity.

315 “In these areas north of the foamed areas, the subsidence inversion is not quite as strong
316 as it is right under the subtropical high. However, SSTs are artificially low, due to general
317 cooling of the hemisphere and enhanced upwelling, driven by anomalously strong winds, and
318 mixing of this anomalously cool surface air within the planetary boundary layer keeps the lowest
319 levels of the atmosphere cool, keeping the marine air inversion base above the lifting
320 condensation level, allowing stratocumulus clouds to form at low altitude, below the base of the
321 inversion. Additionally, since SST is lower than air temperature in the areas of enhanced low
322 clouds, the surface inversion is further maintained as a result of sensible heat flux from the
323 atmosphere to the ocean. Ultimately, the strong inversion often results in more marine layer
324 cloud formation and longer times for the clouds to dissipate. This response is consistent through
325 the 2030-2069 period. This enhanced low-cloud fraction response is similar to the seasonal
326 cycle of marine low clouds around the periphery of the subtropical highs (Wood and Bretherton,
327 2004; Chiang and Bitz, 2005; Wood and Bretherton, 2006; George and Wood, 2010; Mechoso et
328 al., 2014).

329 “The relationship between the strength of the subtropical high, inversion strength and
330 marine cloud prevalence can be elucidated by analogy to the behavior of the very well-observed
331 marine low clouds off of the California coast. The strength of the inversion, and the prevalence
332 of marine low clouds are modulated by the annual cycle with annual maximum low cloud extent
333 in the summer, when the subtropical high is at its strongest.

334 “The increased low cloud fraction response is not seen above the actual G4Foam forced
335 regions despite the cooler SST. The subsidence is so strong in these areas that the base of the
336 inversion falls below the lifting condensation level, and few clouds form.”

337
338 13) Lines 418-421: Please elaborate on “the temperature dependence of precipitation”.
339

340 We have clarified this portion of section 3.2. It is rather evident that with global
341 warming, specific humidity in the tropical planetary boundary layer will increase by 7% K⁻¹,
342 scaling with Clausius-Clapeyron (e.g., Held and Soden, 2006). However, the processes
343 involving precipitation are quite complex and while it is clear that global mean precipitation will
344 increase as global mean temperature increases, there is a wide range of estimates in the literature
345 of how much precipitation will increase per degree of global warming. In the revised
346 manuscript, we refer to a review that collects estimates from the literature of how much
347 precipitation will increase per degree of global warming. They estimate a 1.5%-3% K⁻¹ range.

348 We then report the precipitation change in G4Foam, relative to both G4SSA and RCP6.0
349 and note that while global mean precipitation over land and ocean changes by about 2%-3% per
350 degree of global mean temperature, the changes over land, especially over the tropics, are
351 dramatically different. Precipitation actually increases over land in G4Foam relative to RCP6.0,
352 despite 0.6 K of cooling and there is far more precipitation over land in G4Foam than G4SSA
353 despite G4Foam being only slightly warmer. We’ve clarified the discussion in the revised
354 manuscript.

355
356 *We have also shortened the abstract by one sentence. Line 646-647 added to acknowledgements*
357 *to thank you for your valuable comments.*
358

359 References

360

361 [Held, I. M. and Soden, B. J.: Robust responses of the hydrological cycle to global warming, J.](#)
362 [Climate, 19, 5686–5699, 2006.](#)
363
364 [Neale, R., Richter, J., Park, S., Lauritzen, P., Vavrus, S., Rasch, P. and Zhang, M.: The mean](#)
365 [climate of the Community Atmosphere Model \(CAM4\) in forced SST and fully coupled](#)
366 [experiments, J. Climate, 26, 5150–5168, 2013.](#)
367
368 [Xia, L., Robock, A., Tilmes, S., and Neely III, R. R.: Stratospheric sulfate geoengineering could](#)
369 [enhance the terrestrial photosynthesis rate, Atmos. Chem. Phys., 16, 1479-1489,](#)
370 [doi:10.5194/acp-16-1479-2016, 2016.](#)
371
372
373

**The G4Foam Experiment:
Global Climate Impacts of Regional Ocean Albedo Modification**

Corey J. Gabriel^{1*}, Alan Robock¹, Lili Xia¹, Brian Zambri¹, and Ben Kravitz²

¹Department of Environmental Sciences, Rutgers University, New Brunswick, NJ, USA

²Atmospheric Sciences and Global Change Division, Pacific Northwest National Laboratory,
[Richland](#), Washington, USA

Submitted to *Atmospheric Chemistry and Physics*
Special Issue: The Geoengineering Model Intercomparison Project

September, 2016

Revised [December](#), 2016

*To whom correspondence should be addressed: Corey J. Gabriel, Department of Environmental Sciences, Rutgers University, 14 College Farm Road, New Brunswick, NJ 08901-8551. E-mail: corey@envsci.rutgers.edu.

376

377 **Abstract.** Reducing insolation has been proposed as a geoengineering response to global
378 warming. Here we present the results of climate model simulations of a unique Geoengineering
379 Model Intercomparison Project Testbed experiment to investigate the benefits and risks of a
380 scheme that would brighten certain oceanic regions. The National Center for Atmospheric
381 Research CESM-CAM4-CHEM global climate model was modified to simulate a scheme in
382 which the albedo of the ocean surface is [increased](#) over the subtropical ocean gyres in the
383 Southern Hemisphere. [In theory, this could be accomplished using](#) a stable, nondispersive foam,
384 comprised of tiny, highly reflective microbubbles. [Such a foam has](#) been developed under
385 idealized conditions, [although deployment at a large scale is presently infeasible](#). We conducted
386 three ensemble members of a simulation (G4Foam) from 2020 through 2069 in which the albedo
387 of the ocean surface is [set](#) to 0.15 ([an increase of 150%](#)) over the three subtropical ocean gyres in
388 the Southern Hemisphere, [against a background of](#) the RCP6.0 (representative concentration
389 pathway resulting in +6 W m⁻² radiative forcing by 2100) scenario. [After 2069, geoengineering](#)
390 [is ceased, and the simulation is run for an additional 20 years](#). Global mean surface temperature
391 in G4Foam is 0.6 K lower than RCP6.0, with statistically significant cooling relative to RCP6.0
392 south of 30°N. [There is](#) an increase in rainfall over land, most pronouncedly in the tropics during
393 the June-July-August season, relative to both G4SSA (specified stratospheric aerosols) and
394 RCP6.0. Heavily populated and highly cultivated regions throughout the tropics, including the
395 Sahel, Southern Asia, the Maritime Continent, Central America and much of the Amazon,
396 experience a statistically significant increase in precipitation minus evaporation. The
397 temperature response to the relatively modest global average forcing of -1.5 W m⁻² is amplified
398 through a series of positive cloud feedbacks, in which more shortwave radiation is reflected. The
399 precipitation response is primarily the result of the intensification of the southern Hadley cell, as
400 its mean position migrates northward and away from the Equator in response to the asymmetric
401 cooling.
402

403 1 Introduction

404 1.1 Background

405 The current rate of increase in global mean surface temperature is unprecedented in the
406 last 1,000 years (Marcott et al., 2013). The atmospheric concentration of CO₂ is higher now than
407 at any time in the last 650,000 years (Siegenthaler et al., 2005). It is extremely likely that the
408 warming since 1950 is primarily the result of anthropogenic emission of heat-trapping gases
409 rather than natural climate variability (IPCC, 2013). Motivated by insufficient progress in
410 setting and achieving mitigation targets, [solar radiation management \(SRM\)](#) has been proposed
411 as a method of reducing global mean temperature, thereby ameliorating many of the negative
412 effects of global warming (Crutzen, 2006). The most discussed SRM approach involves
413 injection of sulfur dioxide (SO₂) into the tropical stratosphere. Other suggested SRM
414 geoengineering methods include marine cloud brightening (Jones et al., 2009; Rasch et al., 2009;
415 Latham et al., 2010) and surface albedo modification (Irvine et al., 2010; Cvijanovic et al.,
416 2015). Each of these methods has the potential to cool Earth's surface, but each comes with
417 known potential side effects. For example, Robock (2008, 2014, [2016](#)) enumerated and
418 described specific risks and benefits of stratospheric geoengineering.

419 Here we present a Geoengineering Model intercomparison Project (GeoMIP) testbed
420 experiment (Kravitz et al., 2011, 2016), consisting of the novel implementation of an ocean
421 surface albedo modification scheme in a climate model, which simulates the placement of a
422 reflective foam, consisting of microbubbles, on the ocean surface. RCP6.0 and G4SSA are run
423 with an ocean surface albedo [with](#) a very small diurnal cycle, [and](#) the [daily](#) average albedo is
424 very close to 0.06. [In our experiment, the](#) albedo of the ocean surface is raised from this daily
425 mean of 0.06 to a constant value of 0.15, with no daily cycle, over the subtropical ocean gyres in
426 the Southern Hemisphere, specifically 20°N-20°S, 90°W-170°W (South Pacific), 20°N-20°S,
427 30°W-0°E (South Atlantic) and 20°N-20°S, 55°E-105°E (South Indian) (Fig. 1). Everywhere
428 else, ocean surface albedo in G4Foam is calculated in the same way as in RCP6.0 and G4SSA.
429 It is possible that the absence of a small daily cycle in albedo would result in a slightly different
430 surface energy budget than would occur if the foamed regions exhibited variations in albedo.
431 However, the foamed regions' albedos would likely fluctuate as a function of many things,
432 including some movement of the foam itself, foam interaction with precipitation or aerosols,
433 wind speed, and sun angle. Further study of the properties of the foam, [including](#) in ocean water
434 with some turbulence, could provide information that would allow future modeling of the foam
435 to include albedo fluctuations. This is the G4Foam experiment, which simulates a particular
436 implementation of an idealized form of the technology described by Aziz et al. (2014), where
437 stable, reflective foam suitable for use as SRM in ocean regions with limited nutrients that
438 support little marine life is made in the laboratory.

439 The broad idea of microbubble deployment as a form of SRM is explored by Seitz
440 (2010). Here we only examine the potential benefits and risks of such a scheme, and do not
441 advocate deployment of any form of geoengineering [regardless of its present feasibility](#). Robock
442 (2011) has cautioned against the potential implications of ocean albedo modification as presented
443 by Seitz (2010).

444 Stratospheric sulfate injection (SSI) [is](#) the most discussed form of geoengineering [and](#),
445 [given the current state of research, the most feasible](#) (Dykema et al., 2014, Keith et al., 2014).
446 Implementation of the G4Foam regional ocean albedo modification scheme could be considered
447 with or without concurrent SSI. G4Foam could be used as a potential SSI concurrent scheme
448 aimed at correcting possible [adverse](#) impacts on the hydrological cycle brought about by ongoing
449 SSI. G4Foam is also a potential alternative to SSI with a far different latitudinal distribution of

450 benefits. The focus here is solely on the second scenario, as it allows for the elucidation of the
451 impacts of the G4Foam experiment forcing alone.

452 **1.2 Motivation and Research Question**

453 Is it possible to cool the planet while concurrently maintaining or increasing precipitation
454 in highly populated and heavily cultivated regions, particularly in regions dependent on monsoon
455 precipitation? We begin by determining whether a forcing can be applied in a global climate
456 model (GCM) that will result in the model responding with a northward and landward shift of
457 tropical precipitation needed to achieve our objective. To that end we conducted simulations
458 with The Community Earth System Model 1/Community Atmospheric Model 4 fully coupled to
459 tropospheric and stratospheric chemistry (CESM1 CAM4–Chem) model (Lamarque et al., 2012;
460 Tilmes et al., 2015, 2016). We ran the model with horizontal resolution of $0.9^\circ \times 1.25^\circ$ lat-lon
461 and 26 levels from the surface to about 40 km (3.5 mb), as was done for G4SSA (specified
462 stratospheric aerosol) by Xia et al. (2016).

463 The experiments consisted of three ensemble members of a simulation from 2020-2089 in
464 which the ocean surface albedo is raised as described above from an average of 0.06, which
465 includes a small diurnal cycle of albedo, to a daytime constant 0.15 on the SH subtropical ocean
466 gyres for 50 years, 2020-2069, and then returned to unforced values from 2070-2089 to assess
467 termination. Our hypothesis is that the tropical rain belts will move northward largely as a result
468 of increased moisture convergence over land regions, particularly during Northern Hemisphere
469 (NH) summer (June-July-August, JJA) in NH monsoon regions. Enhanced divergence over the
470 already strong subtropical highs, due to increased subsidence over the increased albedo ocean
471 regions in the subtropical Southern Hemisphere (SH), would help the cooler air from the forced
472 subtropical regions advect throughout the SH troposphere.

473 The asymmetric cooling would force changes in the Hadley Cell, enhancing cross-
474 equatorial flow, which would cool the surface in the NH tropics, especially during JJA, when
475 heat mortality and morbidity is highest. However, despite a reduction in the JJA mean
476 temperature in the tropics, extreme events are responsible for most heat-related mortality and
477 morbidity, and the reduction in the mean temperature does not necessarily mean that there will
478 be a reduction in the type of extreme heat events that cause human tragedy. While Kharin et al.
479 (2007) showed that, in general, temperature extremes track with the mean temperature, this is not
480 always the case. The changes in extreme events may, for example, be greater at high latitudes
481 and the variability of temperatures over land may increase in a warmer climate.

482 Specific to geoengineering, Aswathy et al. (2015) showed that different climate
483 engineering methods produce spatially heterogeneous changes in extreme precipitation and
484 temperature events. They showed that one SRM scheme may be more effective than another in
485 reducing different types of extreme events despite relatively similar global and regional mean
486 responses. In particular, a marine cloud brightening scheme that brightens ocean areas between
487 30°N and 30°S is shown to be less effective in reducing extreme precipitation and temperature
488 events over land than the G3 experiment is.

489 Finally, the resulting cooling of low latitude NH land areas would not dampen the
490 monsoon. The wet season monsoon circulation is initiated and maintained by the moist static
491 energy gradient, not the surface temperature gradient. A wetter, more cloudy land mass will
492 strengthen, not dampen the circulation relative to a warmer, drier continent (Hurley and Boos,
493 2014), especially with a cooler, lower specific humidity environment under the descending
494 branch of the meridional circulation.

495 The strength of this response will be very sensitive to any cloud feedbacks that result
496 from the surface albedo forcing. The basis of this comprehensive hypothesis is described in

497 detail, below, specifically in sections 1.3 and 1.4. The details of the experiment are discussed in
498 detail in section 2.

499 **1.3 Stratospheric geoengineering weakens the hydrological cycle**

500 With global warming, low-level specific humidity will increase by about $7\% K^{-1}$ within
501 the tropical planetary boundary layer. This response will be spatially homogeneous throughout
502 the tropics. However, the precipitation response will be different. Increased moisture
503 convergence in areas that already get a lot of precipitation will result in the “wet getting wetter,”
504 while increased moisture divergence in dry areas will result in the “dry getting drier” (Held and
505 Soden, 2006).

506 The “rich get richer, poor get poorer” paradigm does not hold up in an SRM world, where
507 the response is very different from that under global warming. Based on the results of an
508 observational study, Trenberth and Dai (2007) pointed out the possibility that drought,
509 particularly in the tropics, could result from geoengineering. Tilmes et al. (2013) analyzed the
510 hydrological cycle in most of the GeoMIP participating Coupled Model Intercomparison Project
511 | 5 (CMIP5) (Taylor et al., 2012) models by comparing abrupt $4xCO_2$, piControl, and G1. They
512 | found a robust reduction in global monsoon rainfall, including in the Asian and West African
513 | monsoon regions in G1 relative to both abrupt $4xCO_2$ and piControl. Haywood et al. (2013)
514 | explored the impact of SSI in one hemisphere only and found a movement of the ITCZ away
515 | from the hemisphere that was cooler as a result of the asymmetric SSI.

516 | This consensus about the potential for [less](#) tropical rainfall under a regime of
517 | stratospheric SRM motivates us to identify an alternative or SSI-adjunctive geoengineering
518 | approach that could cool the planet, without reducing monsoon precipitation in highly cultivated
519 | areas.

520 **1.4 Extratropical forcing impacts the position of the ITCZ**

521 Under global warming tropical rainbelts will move toward the hemisphere that warms
522 | more (Chiang and Bitz, 2005, Frierson and Hwang, 2012). [This ITCZ migration was first seen in](#)
523 | [early atmosphere-ocean coupled models. Clouds were prescribed in those models, and when](#)
524 | [clouds were changed in such a way to preferentially cool one hemisphere, the ITCZ responded to](#)
525 | [changes by moving toward the warmer hemisphere.](#) Increasing low cloud cover, and thereby
526 | inducing cooling, in one hemisphere relative to the other caused the tropical rainbelts over the
527 | Pacific Ocean to move toward the other hemisphere (Manabe and Stouffer, 1980). The impacts
528 | of asymmetric heating of the hemispheres became highly relevant during the Sahel drought.
529 | Much of the rainfall deficit during the devastating 20-30 year drought can be attributed to
530 | cooling initiated by increased tropospheric sulfate emissions in the NH (Hwang et al., 2013).
531 | The forced cooling over the NH was enhanced by a positive dynamical feedback in the North
532 | Atlantic Ocean. (Broccoli et al. 2006; Kang et al. 2008) and the ITCZ and associated tropical
533 | rainbelts migrated south. Since the Sahel is at the northern margin of the ITCZs annual
534 | migration, or at the northern terminus of the West African monsoon, southward displacement of
535 | the ITCZ led to a devastating drought (Folland, 1986).

536 Broccoli et al. (2006) diagnosed the energy balance mechanism that causes the ITCZ to
537 | shift in response to asymmetric heating of the extratropics. Using models of varying complexity,
538 | Broccoli et al. (2006) imposed an anomalous cooling of the NH, either via a last glacial
539 | maximum simulation, or via hosing of the North Atlantic. The heating asymmetry causes the
540 | extratropics in the NH to demand more heat and the extratropics in the SH to demand less heat.
541 | Since cross equatorial heat transport is achieved principally via the Hadley Cell, the SH Hadley
542 | Cell strengthens, particularly in austral summer, in response to the NH cooling, and net energy
543 | flow in the upper branch intensifies, redistributing energy into the NH from the relatively warm
544 | SH.

545 | Net flow of energy in the Hadley cell [can be described in terms of](#) the flow of moist static
546 energy, which flows in the direction of the upper troposphere branch of the Hadley Cell. This is
547 because moist static energy is higher at higher altitudes in the troposphere due to the increased
548 contribution of the geopotential energy term overwhelming the moisture and internal energy
549 terms in the moist static energy equation for the high altitude air. Net transport of energy,
550 occurring in the upper branch of the Hadley cell from the SH to the NH, leads to increased
551 moisture advection to the SH in the lower branch of the Hadley Cell. This redistribution of
552 energy causes the ascending branch of the Hadley cell to migrate to the warmer SH where
553 moisture convergence is increased and convective quasi-equilibrium is achieved under the
554 relatively narrow poleward shifted ascending branch of the stronger SH winter Hadley Cell.
555 This mechanism leads to the southward-displaced tropical rain belts (Broccoli et al., 2006).

556 This result is consistent with Lindzen and Hou (1988), who used a relatively simple
557 model to show that even a small movement of maximum heating poleward into one hemisphere
558 causes great asymmetry in the Hadley Cell, with the winter cell intensifying tremendously and
559 the summer cell becoming rather modest. More recent work continues to elucidate the
560 mechanism of extratropical forcing of the ITCZ (Kang et al. 2008). The ocean also plays a vital
561 role in pushing the ITCZ into the warmer hemisphere (Xie and Philander, 1994).

562 GCM results confirm this mechanism and connect the changes due to northward
563 displacement of the ITCZ with the onset of active periods in the Asian summer monsoon (Chao
564 and Chen 2001). It is evident that a geoengineering technique that could preferentially cool the
565 SH could shift the tropical rain bands northward. However, in a GCM there are clouds. How
566 would clouds respond in the hemisphere cooled by geoengineering? Would clouds change in the
567 area being directly cooled? Would a cooling of the subtropics either directly, or indirectly via
568 eddy flux from the artificially cool high latitudes, cause an increase in subtropical subsidence?
569 Would this increase in the sinking of air above the intensified subtropical highs cause water
570 vapor to be trapped in the lower troposphere, forming low clouds and suppressing water vapor
571 mixing into the free troposphere, where the water vapor may instead be used up in formation of
572 high clouds, which tend to reduce outgoing longwave radiation? Informed by these established
573 diagnostic mechanisms associated with the impacts of asymmetric heating of the hemispheres,
574 we seek to concurrently cool the entire SH and the NH tropics, modestly cool the NH
575 extratropics and, most importantly, induce an anomalous overturning circulation and redistribute
576 rainfall from ocean to land and from south to north across the tropics.

577 **2. Methods**

578 **2.1 Design of experiment and model configuration**

579 Figure 1 shows the regions selected for albedo enhancement. These regions were chosen
580 because of their low cloud fraction, low wind speeds, weak currents, and lack of biological
581 productivity.

582 We used the Community Land Model (CLM) version 4.0 with prescribed satellite
583 phenology (CLM4SP) instead of the version of CLM with a carbon–nitrogen cycle, coupled with
584 CAM4–chem. Vegetation photosynthesis is calculated under the assumption of prescribed
585 phenology and no explicit nutrient limitations (Bonan et al., 2011, Xia et al., 2016). Dynamic
586 vegetation is not turned on in this study. The ocean model does not include any biogeochemical
587 responses.

588 The fundamental question we wish to answer concerns representation of the physical
589 processes that lead to realistic simulation tropical precipitation. The Asian monsoon is of great
590 importance in that investigation. Fortunately, monsoon processes and regimes are depicted well
591 in our atmospheric component, CAM4 (Meehl et al., 2012). Some important features of CAM4
592 that illustrate its very good monsoon representation include the amount and location of

593 precipitation over the southern Tibetan Plateau and over the Western Ghats (a mountain range
594 near the west coast of south India). This is improved when compared to earlier versions of the
595 model. The rain shadow leeward of this range is often not resolved by GCMs, however CAM4
596 shows some evidence of this rain shadow. These changes related to orography and horizontal
597 resolution are important and likely generalize to similar land surface features outside of India,
598 where model biases have not been as carefully studied as they have been in heavily populated
599 southern India. This improvement can be attributed to the CCSM4 finite-volume dynamical
600 core, which replaces the spectral version of the CCSM3 and the interconnected higher horizontal
601 resolution (Neale et al., 2013). Additionally, large-scale features are improved. For example,
602 the representation of the ITCZ during NH winter southward migration over the maritime
603 continent is improved (Meehl et al., 2011).

604 | There is an important process associated with monsoon precipitation, however, that [may](#)
605 | [be imperfectly simulated](#) across [many](#) CMIP5 GCMs. Zonal mean absorbed shortwave radiation
606 | is too high over the southern ocean (Kay et al., 2016). This cloud problem leads to a warmer
607 | Southern Ocean, which leads to anomalous SH atmospheric eddy flux to the subtropics from the
608 | extratropics, potentially damping the cooling response of our negative surface radiative forcing
609 | in the subtropical oceans. The effect of a transfer of heat from the SH extratropics into the
610 | Hadley Cell already causes a relatively weak negative bias in the amount of interhemispheric
611 | heat transport from the south to north. Therefore, the manifestation of this bias in G4Foam
612 | would be to partially offset our imposed cooling, lessening the need for interhemispheric energy
613 | transport to the SH and suppressing the surface return flow of moisture advection into the NH.
614 | Lower than observed interhemispheric energy transport would be associated with a weaker Asian
615 | monsoon. However, this feature is equally present in our G4Foam experiment and [the](#)
616 | [comparison](#) experiments [G4SSA and RCP6.0](#), so [is unlikely to appreciably](#) affect the differences.

617 | We compare G4Foam to two experiments. First is a specific sulfate injection scenario,
618 | G4 Specified Stratospheric Aerosol (G4SSA; Xia et al., 2016). They used a prescribed
619 | stratospheric aerosol distribution roughly analogous to annual tropical emission into the
620 | stratosphere (at 60 mb) of 8 Tg SO₂ yr⁻¹ from 2020 to 2070. This produces a radiative forcing of
621 | about -2.5 W m⁻². The G4SSA forcing ramps down from 2069-2071 and then continues without
622 | additional forcing from 2072-2089. In G4SSA tropospheric aerosols are not affected by the
623 | prescribed stratospheric aerosols. Therefore we cannot evaluate how stratospheric aerosols
624 | would actually fall out and impact the chemistry, dynamics and thermodynamics of the
625 | troposphere from this experiment. Neely et al. (2015) offers more detail on the prescription of
626 | stratospheric aerosols in CAM4-Chem. The second [simulation for comparison](#), which serves as
627 | the reference simulation, for both G4Foam and G4SSA is the Representative Concentration
628 | Pathway 6.0 (RCP6.0) (Meinshausen et al., 2011) from 2004 to 2089. We have run three
629 | ensemble members each for G4Foam, G4SSA, and RCP6.0.

630 | 2.2 Ocean albedo enhancement approach

631 | [A plausible technology now exists](#) to make quantities of long lasting foam, or engineered
632 | microbubbles to enhance ocean albedo. [Ocean albedo modification gained attention when](#)
633 | Seitz (2010) [suggested](#) that since air-water and air-sea interfaces are similarly refractive,
634 | dispersing microbubbles onto the surface of the ocean would reflect sunlight in much the same
635 | way as cloud droplets do. While engineering refractive or stable foams is commonly done and
636 | applied in both food science and firefighting, engineering a stable and refractive foam
637 | appropriate for a geoengineering scheme appeared fanciful until Aziz et al. (2014) produced a
638 | long lasting refractive foam made with biodegradable and non-toxic additives. Aziz et al.
639 | identified foam lifetime of three months or more per microbubble as lasting long enough that the
640 | input of energy to create the microbubbles would not be prohibitive. After experimenting with

641 protein-only solutions, Aziz et al. (2014) added high methyl ester pectin to type A gelatin and
642 created a foam in salt water, which was still intact and stable at the cessation of the experiment
643 after 3 months. The reflectance of the foam was about 50%, which is comparable to that of
644 whitecaps. The creation of these stable microbubbles makes enhancing ocean albedo in this
645 manner “feasible” (Aziz et al. 2014). However, there are a number of other potential risks
646 associated with microbubble deployment, even if the feasibility issues are set aside. Robock
647 (2011) pointed out that vertical mixing in the ocean, changes in ocean circulation, impacts on
648 photosynthesis, and risks to the biosphere could all impair the efficacy of this geoengineering
649 approach. Robock (2011) also pointed out that a cooler ocean would serve as a more effective
650 CO₂ sink, helping to offset the CO₂ increase that comes about as a feedback of warming. Other
651 potentially attractive attributes of this technique include the possibility that it could be deployed
652 exclusively in the 20% of the world’s oceans that are not biologically active (Aziz et al. 2014)
653 and therefore have little impact on the biosphere, and that there would be no risk to ozone in the
654 stratosphere.

655 **3 Results**

656 The following results compare the G4Foam climate with the climates in G4SSA and
657 RCP6.0 averaged over the period 2030-2069. While G4Foam and G4SSA forcing commences in
658 2020, the first ten years of both experiments are a period of transition. For that reason 2020-
659 2029 is discarded from our comparisons. We analyze mainly annual average and JJA results,
660 since JJA is meteorological summer in the NH and using JJA facilitates comparison with
661 G4SSA, which reports results in terms of JJA (Xia et al., 2016).

662 **3.1 Temperature and cloud response**

663 The primary purpose of G4Foam is to assess the possibility of reducing global mean
664 surface temperature without reducing monsoon precipitation. The G4Foam simulations reduce
665 global mean surface temperature relative to RCP6.0 by 0.60 K and global mean land surface
666 temperature by 0.51 K relative to RCP6.0. In JJA, G4Foam is 0.70 K cooler than RCP6.0 over
667 land in the tropics, 20°S-20°N, during JJA (Table 1).

668 These temperature changes in G4Foam, relative to RCP6.0, result from an all-sky top-of-
669 atmosphere forcing of -1.5 W m⁻² (global, year-round), and -1.9 W m⁻² in the tropics during JJA
670 only (Figure 2). This JJA cooling in the tropics is of particular importance due to the dense
671 population and heavy agricultural demand in the tropics, particularly north of the equator.

672 G4Foam does not achieve the same amount of cooling as G4SSA, which would reduce
673 global mean surface temperature by 0.92 K. All-sky top-of-atmosphere shortwave flux in G4SSA
674 is reduced by 2.7 W m⁻² as compared to RCP6.0. In terms of global mean clear-sky top-of-
675 atmosphere shortwave flux, relative to RCP6.0, G4Foam applies only 38% of the forcing that is
676 applied in G4SSA (Figure 3). The G4Foam forcing is more efficient in reducing temperature
677 than G4SSA largely because there is an additional 1.1 W m⁻² of net cloud forcing in G4Foam
678 relative to G4SSA (Figure 2b).

679 Figure 4 shows a comparison of the spatial distribution of surface temperature changes
680 between G4Foam and G4SSA and between G4Foam and RCP6.0 between 2030-2069. Over the
681 SH ocean gyres that were brightened (Fig. 1), we see a very robust cooling, reaching 2 K at the
682 center of the South Pacific foamed region. However, the cooling mixes rather well throughout
683 the SH. Cross equatorial flow and changes in the Hadley Cell transmit this cooling into the NH
684 tropics through the mechanisms described in section 1.4, above. Some of this cooling in the NH
685 tropics is then transmitted to the NH extratropics.

686 G4Foam is significantly cooler ($p < 0.05$) than RCP6.0 in almost all locations south of
687 30°N, in mid latitude NH continental regions windward of the Atlantic and Pacific, and at very
688 high latitudes. Figure 4d shows that G4Foam is less effective in cooling extratropical NH land

689 regions during JJA. This is reasonable, since continental heating in the NH JJA season is more
690 dominated by local heating than the other seasons, in which meridional energy transport plays a
691 larger role. Figures 4a and 4c show that G4SSA is more effective over NH continents than
692 G4Foam. A key weakness of G4Foam, if implemented alone, would be its failure to adequately
693 reduce human suffering induced by heat stress in NH mid-latitudes during the summer as a result
694 of ongoing global warming.

695 Since the G4Foam forcing alone, with the amplitude of the current experiments, would be
696 insufficient to achieve any of the objectives of the G4Foam experiment, positive feedbacks that
697 enhance cooling and circulation responses must be triggered by the G4Foam forcing to enhance a
698 resulting cooler, wetter climate. Figure 5 shows change in low cloud fraction both year-round
699 and in the JJA season. The largest change is in the northern half of the regions where foam is
700 applied, and the area to the north of those foamed regions. The changes in low clouds in these
701 regions are both large and statistically significant.

702 The low cloud fraction increase in the three areas to the north and northeast of the
703 G4Foam-forced subtropical surface regions is likely due to a stronger than normal trade wind
704 inversion (TWI). The inversion develops when warm air is trapped above the atmospheric
705 mixed layer due to large-scale subsidence and surface mixing of cooler air above these relatively
706 low SST regions. The increase in low cloud fraction does not occur over the entire downwind
707 area because SSTs increase from east to west, causing a change in the lower troposphere from
708 east to west. Moving west, the stratocumulus layer, which is trapped under the inversion base,
709 decouples from the mixed layer in the lower troposphere. The surface warming triggers more
710 turbulence within the planetary boundary layer, which allows for enhanced cumulus mixing in
711 the cloud layer, which entrains dry air, and the marine stratocumulus layer evaporates.

712 The subtropical high-pressure systems are stronger in G4Foam, due to the stronger than
713 normal Hadley Cell, which enhances subsidence throughout the subtropics. Typically, a
714 subsidence inversion is strongest over the center of the subtropical anticyclones, over cold
715 currents (particularly the Peru Current), and over cooler than normal waters, which are subjected
716 to enhanced upwelling in large part by trade winds on the periphery of the subtropical highs
717 (DeSzoeke et al., 2016). The TWI becomes weaker and its base increases in height with distance
718 towards the west and towards the equator as SSTs increase. This pattern is particularly evident
719 in the Pacific, due to the larger geographical extent of the forced area.

720 Specifically, under G4Foam conditions, the increased low cloud fraction areas are the
721 result of the combination of enhanced large-scale subsidence (stronger Hadley cell) and a cooler
722 than normal ocean surface. The cooler than normal surface waters are due to general cooling
723 throughout the SH, as well as an increase in wind-driven upwelling over these areas of increased
724 low cloud fraction, which are already prone to upwelling, large fraction of low clouds and high
725 relative humidity.

726 In these areas north of the foamed areas, the subsidence inversion is not quite as strong as
727 it is right under the subtropical high. However, SSTs are artificially low, due to general cooling
728 of the hemisphere and enhanced upwelling, driven by anomalously strong winds, and mixing of
729 this anomalously cool surface air within the planetary boundary layer keeps the lowest levels of
730 the atmosphere cool, keeping the marine air inversion base above the lifting condensation level,
731 allowing stratocumulus clouds to form at low altitude, below the base of the inversion.
732 Additionally, since SST is lower than air temperature in the areas of enhanced low clouds, the
733 surface inversion is further maintained as a result of sensible heat flux from the atmosphere to
734 the ocean. Ultimately, the strong inversion often results in more marine layer cloud formation
735 and longer times for the clouds to dissipate. This response is consistent through the 2030-2069
736 period. This enhanced low-cloud fraction response is similar to the seasonal cycle of marine low

737 [clouds around the periphery of the subtropical highs \(Wood and Bretherton, 2004; Chiang and](#)
738 [Bitz, 2005; Wood and Bretherton, 2006; George and Wood, 2010; Mechoso et al., 2014\).](#)

739 [The relationship between the strength of the subtropical high, inversion strength and](#)
740 [marine cloud prevalence can be elucidated by analogy to the behavior of the very well-observed](#)
741 [marine low clouds off of the California coast. The strength of the inversion, and the prevalence](#)
742 [of marine low clouds are modulated by the annual cycle with annual maximum low cloud extent](#)
743 [in the summer, when the subtropical high is at its strongest. The increased low cloud fraction](#)
744 [response is not seen above the actual G4Foam forced regions despite the cooler SST. The](#)
745 [subsidence is so strong in these areas that the base of the inversion falls below the lifting](#)
746 [condensation level, and few clouds form \(Fig. 5\).](#)

747 Another striking G4Foam feature is the large and statistically significant increase in low
748 clouds over land across central Africa, the Middle East and Southeast Asia. These low clouds
749 are coincident with the large cooling in Africa and the Middle East, particularly during the JJA
750 season relative to both G4SSA and RCP6.0 (Figs. 5c, 5d). These are very hot areas and heat
751 related mortality and morbidity are of great concern. A similar increase in low clouds is evident
752 in the tropical eastern Pacific. This is coincident with the mean northward displacement of the
753 ITCZ in G4Foam with respect to G4SSA and RCP6.0, not with any changes in the El Niño-
754 Southern Oscillation (ENSO).

755 In G4Foam, clouds are the key to changing the radiation budget in the tropics. In
756 G4Foam there is a change in shortwave cloud forcing of -2.32 W m^{-2} annually and -2.59 W m^{-2}
757 during JJA, relative to G4SSA. Only very small increases in longwave cloud forcing of 0.42 W m^{-2}
758 annually, and 0.07 W m^{-2} in JJA counter this negative forcing. The overall change in cloud
759 radiative forcing in the tropics is -1.90 W m^{-2} annually and -2.52 W m^{-2} during JJA. Relative to
760 RCP6.0, in G4Foam there is a change in shortwave cloud forcing of -0.68 W m^{-2} annually
761 and -0.89 W m^{-2} during JJA, relative to RCP6.0. Small increases in longwave cloud forcing of
762 0.40 W m^{-2} annually, and 0.28 W m^{-2} in JJA counter part of this negative forcing. The overall
763 change in cloud radiative forcing in G4Foam in the tropics is -0.49 W m^{-2} annually and -0.61 W m^{-2}
764 during JJA when compared to RCP6.0

765 Total cloud fraction is shown in Fig. 6. Figs. 6c and 6d are particularly striking in
766 showing the increase in clouds over Africa and Southeast Asia during the JJA wet monsoon
767 season in those regions. Under G4Foam, these regions generally experience cloudier and cooler
768 summers relative to RCP6.0 and are cloudier and only very slightly warmer on average
769 compared to G4SSA. Some parts of the Sahel and the Middle East are actually slightly cooler in
770 G4Foam than RCP6.0. These changes in temperature and cloudiness play a key role in the
771 changes in the hydrological cycle under G4Foam, which we discuss next.

772 **3.2 Hydrological Cycle Response**

773 Relative to G4SSA, precipitation in G4Foam over land in the tropics increases by 3.2%
774 on an annual mean basis and by 3.9% during JJA (Table 1). Tropical precipitation in G4Foam
775 over land in the tropics increases by 1.4% on an annual mean basis and by 2.02% during JJA,
776 when compared to RCP6.0. Each of these changes is statistically significant ($p < 0.05$).
777 Regarding the temperature change relative to G4SSA, G4Foam is only about 0.3 K warmer in
778 the tropics. Precipitation is expected to increase by between $1.5\% \text{ K}^{-1}$ and $3.0\% \text{ K}^{-1}$ as global
779 mean temperature increases (Emori and Brown, 2005). The temperature difference between
780 G4Foam and G4SSA can explain only a fraction of the precipitation increase. The statistically
781 significant increase in land-only precipitation in the tropics in G4Foam relative to RCP6.0 occurs
782 in a climate in which RCP6.0 is between 0.6 K and 0.7 K warmer than G4Foam, depending on
783 the season. Over the tropical oceans, in G4Foam, precipitation is reduced by 0.4% on an annual

784 mean basis and reduced by 0.3% during JJA relative to G4SSA. There is a decrease of 2.6% on
785 an annual mean basis and a decrease of 2.5% during JJA relative to RCP6.0.

786 Globally, over land, the precipitation response is similar to that in the tropics during JJA,
787 but the magnitude of precipitation change is a bit less. Precipitation is statistically significantly
788 increased over land in G4Foam relative to RCP6.0 by about 0.5%, despite G4Foam being cooler
789 than RCP6.0. Precipitation is statistically significantly increased in G4Foam relative to G4SSA
790 over land by 3.5%, despite G4Foam only being 0.3K warmer than G4SSA.

791 The overall global precipitation difference between G4Foam and G4SSA or RCP6.0
792 when land and ocean are combined and all seasons and all latitudes are included is relatively
793 small, and close to the 1.5% K⁻¹ to 3% K⁻¹ range of precipitation increase with temperature
794 identified by Emori and Brown (2005). Globally, G4Foam is warmer than G4SSA by 0.3 K and
795 there is 0.61% (2.1% K⁻¹) more precipitation. G4Foam is cooler than RCP6.0 by 0.6 K and drier
796 by 1.9% (3.1% K⁻¹).

797 The spatial pattern of precipitation changes is shown in Fig. 7. Precipitation is greatly
798 reduced over the ocean, particularly in the SH, relative to both G4SSA and RCP6.0. Changes in
799 precipitation poleward of 40° latitude in either hemisphere are largely due to the temperature
800 dependence of precipitation. The changes in the SH subtropics are dominated by the shortwave
801 forcing applied over the ocean gyres, which reduces both evaporation and precipitation in those
802 areas.

803 The changes in precipitation in the tropics are driven by [a northward shift in the ITCZ](#).
804 Large precipitation anomalies occur in a narrow band north of the equator and smaller positive
805 anomalies occur in broader regions, primarily over NH monsoon regions. Importantly, we see a
806 statistically significant increase in monsoon precipitation over the Sahel, the Middle East, the
807 Indian subcontinent as well as southwest Asia and the maritime continent on an annual mean
808 basis in G4Foam relative to G4SSA (Figure 7a). Relative to RCP6.0, these changes are not
809 statistically significant over the Indian subcontinent or southwest Asia, but there are only very
810 isolated and small areas in these regions in which there is any precipitation reduction, either on
811 the annual mean or during JJA. Therefore, over much of heavily populated southern Asia, east
812 of the Arabian Sea, G4Foam will be cooler than RCP6.0 without any notable [mean](#) precipitation
813 differences. Most of these areas are expected to receive more rainfall as the planet warms. [If](#)
814 [this excess rainfall is not desirable in areas that are already wet, these results suggest that](#)
815 [weakening the hydrological cycle would require that](#) G4Foam would have to be combined with
816 an additional geoengineering technique, such as stratospheric SRM.

817 Relative to both G4SSA and RCP6.0, there is a great deal more precipitation all year and
818 particularly during JJA over central America, the northern Amazon, much of Africa, parts of the
819 Arabian peninsula and the maritime continent. This response is more robust than the response
820 over Southeast Asia due to the more direct dependence of rainfall in these regions on ITCZ
821 position than in Southeast Asia, where the monsoon is also driven by numerous local and remote
822 factors, including ENSO and the Indian Ocean Dipole.

823 Although these G4Foam simulations are enhance rainfall over [many](#) heavily populated
824 and highly cultivated regions, particularly in the tropics, there are regions that would [receive less](#)
825 [precipitation and experience a decrease in P-E](#) under this regime. Precipitation patterns for
826 islands in the South Pacific are largely governed by the position and strength of the South Pacific
827 Convergence Zone (SPCZ), which changes substantially under G4Foam due in part to the
828 cooling and to the movement of gradients of temperature and pressure. Precipitation deficits
829 over Madagascar and some regions in Africa and South America exceed 10%.

830 While the changes in precipitation are important and useful in describing the climate
831 response in G4Foam, the change in precipitation minus evaporation between G4Foam and

832 | G4SSA or RCP6.0 is more relevant to [total available moisture](#). Figure 8 shows precipitation
833 | minus evaporation. Specifically Fig. 8a shows that precipitation minus evaporation in G4Foam
834 | is increased, and this increase is significant relative to G4SSA, across the Sahel, all of South
835 | Asia, the Maritime Continent, Central America and the northern Amazon. These are all heavily
836 | populated regions that are heavily cultivated. Figure 8b shows a similar pattern, albeit with the
837 | regions with significantly higher P-E is slightly suppressed in coverage, when G4Foam is
838 | compared to the warmer RCP6.0 rather than G4SSA. Figures 8c and 8d show changes in P-E
839 | during JJA, the NH wet monsoon season, when water is likely needed the most. Due to
840 | variability in the monsoon, there is more heterogeneity in the JJA response than the annual
841 | response, particularly across Southeast Asia. The P-E gain, driven by a combination of increased
842 | precipitation, lower temperature and increased cloudiness in these heavily cultivated regions,
843 | could be an important benefit of G4Foam. However, G4Foam increased precipitation to levels
844 | that exceed that simulated in RCP6.0.

845 | Figure 9 shows the differences of annual cycles from 2030-2069 for zonal mean
846 | precipitation, zonal mean precipitation minus evaporation, and zonal mean precipitable water
847 | between G4Foam and G4SSA and between G4Foam and RCP6.0. They illustrate the northward
848 | displacement of the ITCZ, with positive precipitation anomalies progressing poleward as the
849 | boreal summer monsoon progresses. Figure 9f shows the difference in the zonal mean annual
850 | cycle for column integrated precipitable water between G4Foam and RCP6.0. The striking
851 | feature here is that zonal mean precipitation is higher at key latitudes in the tropics, despite zonal
852 | mean column integrated precipitable water being much lower at the same latitude.

853 | In Fig. 10, we quantify the impacts on agriculture by looking at the photosynthesis rate
854 | anomalies between G4Foam and RCP6.0. There are small, but statistically significant increases,
855 | in photosynthesis rate in G4Foam relative to RCP6.0 in much of Southeast Asia. The most
856 | dramatic changes occur in Central America and parts of the northern Amazon, where the high
857 | CO₂, relatively cool and very wet conditions promote agriculture.

858 | **4 Discussion**

859 | This paper is an analysis of a geoengineering climate model experiment. Although for
860 | this experiment, global warming is reduced without [seriously affecting](#) precipitation, as was
861 | found in previous stratospheric aerosol implementations, this does not argue for the
862 | implementation of climate engineering. Any such decisions will need to balance all the risks and
863 | benefits of such implementation, and compare them to those from other possible responses to
864 | global warming.

865 | **4.1 Summary**

866 | G4Foam would reduce global mean surface temperature relative to RCP6.0 by 0.6 K for
867 | the 40-year period starting 10 years after the implementation of geoengineering. Clear sky top of
868 | atmosphere net shortwave flux is reduced by 1.5 W m⁻² in G4Foam relative to RCP6.0. This is
869 | achieved primarily by the shortwave forcing over the subtropical SH ocean gyres. Before
870 | accounting for feedbacks, temperature is more sensitive to the forcing applied in G4Foam than
871 | G4SSA. However, global mean surface temperature in G4SSA 0.3 K lower than G4Foam
872 | because of a larger change in all-sky top of atmosphere net shortwave flux (Fig. 3).
873 | Additionally, the latitudinal distribution of temperature reduction is different in G4Foam than in
874 | G4SSA. G4SSA is most effective in cooling the NH continents, while G4Foam most effectively
875 | | cools the surface south of around 30°N (Fig. 4).

876 | Precipitation over land globally, in the tropics, during JJA globally, and during JJA in the
877 | tropics is statistically significantly increased in G4Foam relative to both G4SSA and RCP6.0
878 | (Fig. 7). The increase in precipitation in G4Foam relative to RCP6.0 is very likely undesirable in
879 | areas that already receive a lot of rainfall. The combination of cooling and increased

880 precipitation over land in the tropics results in a statistically significant increase in precipitation
881 minus evaporation on an annual mean basis over Central America, the Northern Amazon, the
882 Sahel, the Indian Subcontinent, the Maritime Continent and Southeast Asia in G4Foam relative
883 to G4SSA (Fig. 8). All of these areas are very densely populated and heavily cultivated. Water
884 scarcity is a major issue in many of these areas and G4Foam describes a climate model response
885 in which there is global cooling, but higher P-E is modeled for many regions, some of which are
886 in need of greater water supply. However, in order to assess actual changes in water supply, it
887 would be necessary to analyze extreme events, as well as the economic and policy issues that
888 ultimately determine the allocation of water resources in a given region.

889 Finally, both the changes in the spatial pattern and magnitude of changes in temperature
890 and precipitation are far too large to be explained by the forcing alone. Instead, much of the
891 temperature and hydrological response is the result of powerful cloud feedbacks and changes in
892 the tropical meridional overturning circulation induced by the placement of the ocean albedo
893 forcing.

894 **4.2 The hydrological response**

895 The dominant cause of the G4Foam hydrological response is the intensification of the
896 southern Hadley Cell and the northward migration of the ITCZ in response to the asymmetric
897 forcing. However, the precipitation response is not zonally homogeneous, as the regional and
898 local mechanisms are also important to the distribution of precipitation.

899 First, we address the increase in precipitation over Central America. For this, we turn to
900 literature concerning the decline of Mayan civilization in Central America. Summer insolation
901 in the NH began to decrease about 5,000 years ago. The ITCZ migrated southward. This
902 southward shift caused rainfall to decrease in the crucial summer growing season. Long
903 droughts and eventually water shortages contributed to the civilization's decline (Poore et al.,
904 2004). In G4Foam, the ITCZ moves northward and the areas in which Mayan civilization
905 flourished, including Belize, Guatemala and parts of Mexico, once again receive a great deal
906 more precipitation. This response is strong and consistent in each ensemble member (Figs. 6-8).

907 The long mid-to-late 20th century Sahel drought was primarily caused by the ITCZ being
908 pushed southward by preferential cooling of the NH (Folland, 1986). In G4Foam, the reverse is
909 true. SH cooling pushes the ITCZ north, which generally explains the G4Foam precipitation
910 increase in the Sahel.

911 A surprising finding is that portions of the Arabian Peninsula equatorward of 20°S
912 experience precipitation increases of up to 1 mm day⁻¹ during the JJA season. However, this
913 northward migration of boreal summer precipitation is evident in the paleoclimate record.
914 Evidence of such precipitation is found in Fleitmann et al. (2003), who showed changes in $\delta^{18}\text{O}$
915 in cave stalagmites in Oman, which indicate increased rainfall in Oman under the influence of
916 northward movement of the ITCZ over the Indian Ocean in periods of relative warmth in the NH
917 relative to the SH.

918 Changes in precipitation over the Maritime Continent are partially attributable to large-
919 scale convergence and rising air in those regions, as they lie longitudinally between G4Foam
920 forcing zones where subsidence is enhanced. However, the Indian Ocean Dipole (IOD) (Cai et
921 al., 2012; Chowadry et al., 2012) and Subtropical Indian Ocean Dipole (SIOD) phenomena
922 discussed below are more likely the key drivers of the precipitation response over the Maritime
923 continent.

924 In its positive phase, the SIOD features anomalously warm SSTs in the southwestern
925 Indian Ocean, east and southeast of Madagascar, and cold anomalies of SST west of Australia.
926 Stronger winds prevail along the eastern edge of the SH subtropical high over the Indian Ocean,
927 which becomes intensified and shifted slightly to the south during positive SIOD events. This

928 results in more evaporation over the eastern Indian Ocean, which cools SSTs in the Indian Ocean
929 east of Australia (Suzuki et al., 2004). In the SIOD negative phase, the opposite is true. There is
930 cooler water in the southwest Indian Ocean, near Madagascar and warmer waters to the east,
931 near Australia (Behera et al., 2001; Reason, 2001).

932 The negative phase of the SIOD features more precipitation in western Australia and the
933 Maritime Continent. This negative SIOD phase is consistent with the SST pattern in the Indian
934 Ocean forced by G4Foam. Therefore, the negative SIOD like mean state in G4Foam appears to
935 play a role in the enhanced rainfall in Northwestern Australia and the Maritime Continent.

936 Based on both local and global changes in circulation, we expected a very large increase
937 in the strength of the Indian Monsoon. In addition to the planetary scale changes associated with
938 the ITCZ and the Hadley cell, the position of the semi-permanent high in the subtropical
939 Southern Indian Ocean also plays a large role in modulating the Indian summer monsoon.
940 Negative SIOD events during boreal winter are often followed by strong Indian summer
941 monsoons. During a negative SIOD event, the subtropical high in the Indian Ocean shifts
942 northeastward as the season shifts from December, January, and February to JJA. This causes a
943 strengthening of the monsoon circulation, intensifying the Hadley Cell locally during the JJA
944 monsoon.

945 A negative IOD is associated with a weakened Asian monsoon and an increase in
946 precipitation over Australia and the Maritime Continent. In G4Foam, advection of cold water in
947 the Somali current into the equatorial western Indian Ocean creates a negative IOD-like response
948 that partially counters the combination of the global scale Hadley cell response and the forced
949 SIOD, dampening the overall increase in the Indian monsoon. This warm west, cold east mean
950 state in the equatorial Indian Ocean resembles a negative IOD mean state and it helps to explain
951 the enhanced precipitation response in the Maritime Continent and the lower than expected
952 increase in precipitation over the Indian subcontinent. The Asian monsoon and precipitation
953 over the Maritime Continent are also governed in part by ENSO. However, no changes in ENSO
954 were evident in G4Foam relative to G4SSA or RCP6.0. There is also no evident response of
955 ENSO amplitude or frequency to any of several different regimes of stratospheric
956 geoengineering (Gabriel and Robock, 2015).

957 **4.3 Caveats**

958 The technology does not presently exist to actually deploy a stable, highly reflective layer
959 of microbubbles on the actual ocean surface. While a stable, highly reflective, nondispersive
960 foam has been developed in a saltwater solution, appropriate for climate engineering, this foam
961 has not been tested outside the laboratory, much less on the surface of a large area of rarely
962 quiescent ocean. The foam has not been immersed in a medium in which bacteria are present,
963 and the interaction between the bacteria and the protein surfactant could damage the layer of
964 microbubbles. Also, even though the diameter of these microbubbles is on the order of 10^{-6} m,
965 the demand for surfactant would likely overwhelm our current production capacity of whatever
966 surfactant is chosen. The research on the engineering required to perform stratospheric
967 geoengineering by sulfate injection is much further along than research of microbubble
968 deployment, which is still in its earliest stages.

969 However, since development of microbubble technology is underway, it is worthwhile to
970 determine how such a technology could be applied in a manner that would address serious
971 climate issues. The progress being made in research associated with stratospheric
972 geoengineering actually enhances the relevance of researching the climate impact of this
973 particular ocean surface geoengineering approach as G4Foam was designed with an eye toward
974 concurrent deployment with stratospheric geoengineering in the event the stratospheric

975 geoengineering were to cause the precipitation deficits that many model studies have shown that
976 it might.

977 More fundamentally, the propriety of any attempt to impose a the G4Foam forcing in an
978 attempt to achieve the modeled G4Foam climate is premised on a value judgment that it is
979 desirable to develop a technology that could redistribute essential resources between nations in
980 an attempt to achieve a net benefit to humanity as a collective when it unknowingly creates a
981 local scarcity of these essential resources. To some extent, making this value judgment is
982 germane and is a prerequisite to the discussion of any form of geoengineering. Even though
983 G4Foam would be successful in increasing P-E in more heavily populated areas, P-E will almost
984 certainly be reduced in remote regions, such as South Pacific islands. Is it ethical to pick
985 winners and losers when the selection process is aimed at increasing the number of winners and
986 decreasing the number of losers? Hypothetically, if G4Foam worked as described in this paper,
987 from a purely consequentialist perspective, and with the sole objective being increased utility for
988 the human collective, G4Foam could be considered beneficial.

989 Finally, this paper is concerned with the climate response to surface albedo changes. We
990 do not examine how placing an actual layer of microbubbles in the ocean would change ocean
991 circulation or impact chemistry and biology in the ocean. Evaluating the changes in the ocean,
992 especially changes in its circulation that are caused by the surface albedo modification, is one of
993 the next issues to explore. The ocean regions we propose to brighten have low biological
994 productivity and weak currents, but the possibility of remote impacts, due to changes in
995 circulation having negative impacts on important ocean regions, is worth considering.

996 4.4 Future research

997 Whether or not a concurrent deployment of stratospheric geoengineering and ocean
998 albedo modification could cool the entire planet while maintaining or enhancing the hydrological
999 cycle, particularly in the tropics, is the next natural step in this research. Such research is
1000 motivated by the need to determine whether some combination of geoengineering techniques can
1001 be used to offset regional climate disparities that using one method of geoengineering alone
1002 could induce.

1003
1004

1005 **Acknowledgments.** We thank two anonymous referees for their valuable comments, which
1006 improved this manuscript. This work is supported by U.S. National Science Foundation (NSF)
1007 grants AGS-1157525, GEO-1240507, and AGS-1617844. Computer simulations were
1008 conducted on the National Center for Atmospheric Research (NCAR) Yellowstone
1009 supercomputer. NCAR is funded by NSF. The CESM project is supported by NSF and the
1010 Office of Science (BER) of the U.S. Department of Energy. [The Pacific Northwest National
1011 Laboratory is operated for the U.S. Department of Energy by Battelle Memorial Institute under
1012 contract DE-AC05-76RL01830.](#)

1013

References

- 1014
1015
1016 Aswathy, V. N., Boucher, O., Quaas, M., Niemeier, U., Muri, H., Mülmenstädt, J., and Quaas, J.:
1017 Climate extremes in multi-model simulations of stratospheric aerosol and marine cloud
1018 brightening climate engineering, *Atmos. Chem. Phys.*, 15, 9593-9610, doi:10.5194/acp-15-
1019 9593-2015, 2015.
1020
1021 Aziz, A., Hailes, H.C., Ward, J.M. and Evans, J.R.G.: Long-term stabilization reflective foams in
1022 seawater. *Royal Society of Chemistry*. 95, 53028–53036. 2014.
1023
1024 Behera, S. K. and Yamagata, T.: Subtropical SST dipole events in the southern Indian Ocean,
1025 *Geophysical Research Letters* 28: 327–330, 2001
1026
1027 Bonan, G. B., Lawrence, P. J., Oleson, K. W., Levis, S., Jung, M., Reichstein, M., Lawrence, D.
1028 M., and Swenson, S. C.: Improving canopy processes in the Community Land Model version
1029 4 (CLM4) using global flux fields empirically inferred from FLUXNET data, *J. Geophys.*
1030 *Res.*, 116, G02014, doi:10.1029/2010JG001593, 2011.
1031
1032 Broccoli, A. J., Dahl, K. A. and Stouffer, R.J.: The response of the ITCZ to Northern
1033 Hemisphere cooling. *Geophys. Res. Lett.*, 33, L01702, doi:10.1029/2005GL024546, 2006.
1034
1035 Cai W., Van Rensch P., Cowan T. and Hendon H.H.: Teleconnection pathways for ENSO and
1036 the IOD and the mechanism for impacts on Australian rainfall, *J. Climate*, 24:3910–3923,
1037 doi:10.1175/2011JCLI4129.1, 2011.
1038
1039 Chao, W.C. and Chen, B.: The origin of the monsoons, *J. Atmos. Sci.*, 58, 3497–3507. 2001.
1040
1041 Chiang, J. C. H. and Bitz, C. M. Influence of high latitude ice cover on the marine Intertropical
1042 Convergence Zone. *Climate Dynamics* 25, 477–496, 2005.
1043
1044 Chowdary J.S., Xie, S-P, Tokinaga, H., Okumura, Y.M., Kubota H., Johnson N. and Zheng X-
1045 T: Interdecadal variations in ENSO teleconnection to the Indo–western Pacific for 1870–
1046 2007, *J. Climate*, 25:1722–1744. doi:10.1175/JCLI-D-11-00070.1, 2012.
1047
1048 Crutzen, P.: Albedo enhancement by stratospheric sulfur injections: A contribution to solve a
1049 policy dilemma?, *Climatic Change*, 77, 211–219, 2006.
1050
1051 Cvijanovic, I., Caldeira, K., and MacMartin, D.G.: Impacts of ocean albedo alteration on Arctic
1052 sea ice restoration and Northern Hemisphere climate, *Environmental Research Letters*, 10,
1053 044020, doi:10.1088/1748-9326/10/4/044020, 2015.
1054
1055 DeSzoeki, S.P., Verlinden, K.L., Yuter, S.E. and Mechem, D.B.: The Time Scales of Variability
1056 of Marine Low Clouds, *J. Climate.*, published online, <http://dx.doi.org/10.1175/JCLI-D-15-0460.1>, 2016.
1057
1058

1059 Dykema J.A., Keith D.W., Anderson J.G., Weisenstein, D.: Stratospheric controlled perturbation
1060 experiment: a small-scale experiment to improve understanding of the risks of solar
1061 geoengineering, *Phil. Trans. R. Soc. A* 372, 20140059, doi:10.1098/rsta.2014.0059, 2014.
1062

1063 Emori, S. and Brown, S.J.: Dynamic and thermodynamic changes in mean and extreme
1064 precipitation under changed climate, *Geophysical Research Letters*, 321,17,
1065 doi:10.1029/2005GL023272, 2005.
1066

1067 Fleitmann, D., Burns, S.J., Mudelsee, M., Neff, U., Kramers, J., Mangini, A., Matter, A., 2003a.
1068 Holocene forcing of the Indian monsoon recorded in a stalagmite from Southern Oman,
1069 *Science*, 300, 1737–1739.
1070

1071 Folland, C. K., Parker, D. E and Palmer, T. N.: Sahel rainfall and worldwide sea temperatures
1072 1901–85, *Nature*, 320, 602–607, 1986.
1073

1074 Frierson, D. M. W. and Hwang, Y-T. Extratropical influence on ITCZ shifts in slab ocean
1075 simulation of global warming, *J. Clim.*, 25, 720–733, 2012.
1076

1077 Gabriel, C. J. and Robock, A.: Stratospheric geoengineering impacts on El Niño/Southern
1078 Oscillation, *Atmos. Chem. Phys.*, 15, 11949-11966, doi:10.5194/acp-15-11949-2015, 2015.
1079

1080 George, R. C. and Wood, R.: Subseasonal variability of low cloud radiative properties over the
1081 southeast Pacific Ocean, *Atmos. Chem. Phys.*, 10, 4047-4063, doi:10.5194/acp-10-4047-
1082 2010, 2010.
1083

1084 Haywood, J. M., Jones, A., Bellouin, N. and Stephenson, D.: Asymmetric forcing from
1085 stratospheric aerosols impacts Sahelian rainfall, *Nat. Clim. Change*, 3(7), 660–665,
1086 doi:10.1038/nclimate1857, 2013.
1087

1088 Held, I. M. and Soden, B. J.: Robust responses of the hydrological cycle to global warming, *J.*
1089 *Climate*, 19, 5686–5699, 2006.
1090

1091 Hurley, J. V. and Boos, W. R.: Interannual variability of monsoon precipitation and local
1092 subcloud equivalent potential temperature. *J. Climate*, 26, 9507–9527, 2013.
1093

1094 Hwang, Y.-T., Frierson, D. M. W. and Kang, S. M.: Anthropogenic sulfate aerosol and the
1095 southward shift of tropical precipitation in the late 20th century, *Geophys. Res. Lett.*, 40,
1096 doi:10.1002/grl.50502, 2013.
1097

1098 IPCC: Summary for Policymakers, in: *Climate Change 2013: The Physical Science Basis.*
1099 *Contribution of Working Group I to the Fifth Assessment Report of the Intergovernmental*
1100 *Panel on Climate Change*, edited by: Stocker, T. F., Qin, D., Plattner, G.-K., Tignor, M.,
1101 Allen, S. K., Boschung, J., Nauels, A., Xia, Y., Bex, V., and Midgley, P. M., Cambridge
1102 University Press, Cambridge, UK and New York, NY, USA, 2013.
1103

1104 Irvine, P. J., Ridgwell, A. and Lunt, D. J.: Climatic effects of surface albedo geoengineering, *J.*
1105 *Geophys. Res.*, 116, D24112, doi:10.1029/2011JD016281, 2011.
1106

1107 | Kang, S. M., Held, I. M., Frierson, D. M. W and Zhao, M.: The response of the ITCZ to
1108 extratropical thermal forcing: Idealized slab-ocean experiments with a GCM, *J.*
1109 *Climate*, 21, 3521–3532, 2008.
1110

1111 Keith, D. W., Duren, R. and MacMartin, D.G.: Field experiments on solar geoengineering: report
1112 of a workshop exploring a representative research portfolio. *Philosophical Transactions of*
1113 *the Royal Society A.*, 372-20140175, 2014.
1114

1115 Kravitz, B., Robock, A., Boucher, O., Schmidt, H., Taylor, K., Stenchikov, G. and Schulz, M.:
1116 The geoengineering model intercomparison project (GeoMIP), *Atm. Sci. Lett.*, 12, 162-167,
1117 doi: 10.1002/asl.316. 201, 2011.
1118

1119 Kravitz, B., Robock, A., Tilmes, S., Boucher, O., English, J. M., Irvine, P. J., Jones, A.,
1120 Lawrence, M. G., MacCracken, M., Muri, H., Moore, J. C., Niemeier, U., Phipps, S. J.,
1121 Sillmann, J., Storelvmo, T., Wang, H., and Watanabe, S.: The Geoengineering Model
1122 Intercomparison Project Phase 6 (GeoMIP6): simulation design and preliminary results,
1123 *Geosci. Model Dev. Discuss.*, 8, 4697–4736, doi:10.5194/gmdd-8-4697-2015, 2015.
1124

1125 Jones A., Haywood, J. and Boucher, O.: Climate impacts of geoengineering marine
1126 stratocumulus clouds, *J. Geophys. Res.*, 114, D10106, doi:10.1029/2008JD011450, 2009.
1127

1128 | Kay J. E., Wall C., Yettella V., Medeiros B., Hannay C., Caldwell P. and Bitz C.: Global
1129 climate impacts of fixing the Southern Ocean shortwave radiation bias in the community
1130 earth system model (CESM), *J. Climate*, doi:10.1175/JCLI-D-15-0358, 2016.
1131

1132 Kharin, V. V., Zwiers, F. W., Zhang, X., and Hegerl, G. C.: Changes in temperature and
1133 precipitation extremes in the IPCC ensemble of Global Coupled Model Simulations, *J.*
1134 *Climate*, 20, 1419– 1444, doi:10.1175/JCLI4066.1, 2007.
1135

1136 Lamarque, J-F., Emmons, L. K., Hess, P. G., Kinnison, D. E., Tilmes, S., Vitt, F., Heald, C. L.,
1137 Holland, E. A., Lauritzen, P. H., Neu, J., Orlando, J. J., Rasch, P. J., and Tyndall, G. K.:
1138 CAM-chem: description and evaluation of interactive atmospheric chemistry in the
1139 Community Earth System Model, *Geosci. Model Dev.*, 5, 369–411, doi:10.5194/gmd-5-369-
1140 2012, 2012.
1141

1142 Latham, J., Bower, K., Choulaton, T., Coe, H., Connoly, P., Cooper, G., Craft, T., Foster, J.,
1143 Gadian, A., Galbraith, L., Iacovides, H., Johnston, D., Launder, B., Leslie, B., Meyer, J.,
1144 Neukermans, A., Ormond, B., Parkes, B., Rasch, P., Rush, J., Salter, S., Stevenson, T.,
1145 Wang, H., Wang, Q., and Wood, R.: Marine cloud brightening, *Phil. Trans. R. Soc. A*, 370,
1146 4217–4262, doi:10.1098/rsta.2012.0086, 2012.
1147

1148 Manabe, S. and Stouffer, R. J.: Sensitivity of a global climate model to an increase of CO₂
1149 concentration in the atmosphere. *J. Geophys. Res.* 85, 5529–5554, 1980.
1150

1151 Mechoso, C., Wood, R., Weller, R., Bretherton, C. S., Clarke, A., Coe, H., Fairall, C., Farrar, J.
1152 T., Feingold, G. and Garreaud, R.: Ocean-cloud-atmosphere-land interactions in the
1153 southeastern Pacific: The VOCALS Program, *Bull. Amer. Meteor. Soc.*, 95, 357-375, 2014.
1154

1155 Meehl, G. A., Arblaster, J. M., Caron, J. M., Annamalai, H., Jochum, M., Chakraborty, A., and
1156 Murtugudde, R.: Monsoon regimes and processes in CCSM4. Part I: The Asian-Australian
1157 Monsoon, *J. Climate*, 25, 2583–2608, 2012.
1158

1159 Meinshausen, M., Smith, S. J., Calvin, K., Daniel, J. S., Kainuma, M. L. T., Lamarque, J.-F.,
1160 Matsumoto, K., Montzka, S. A., Raper, S. C. B., Riahi, K., Thomason, A., Velders, G. J. M.,
1161 and van Vuuren, D. P. P.: The RCP greenhouse gas concentrations and their extension from
1162 1765 to 2300, *Climatic Change*, 109, 213– 241, doi:10.1007/s10584-011-0156-z, 2011.
1163

1164 | Neale, R., Richter, J., Park, S., Lauritzen, P., Vavrus, S., Rasch, P. and Zhang, M.: The mean
1165 climate of the Community Atmosphere Model (CAM4) in forced SST and fully coupled
1166 experiments, *J. Climate*, 26, 5150–5168, 2013.
1167

1168 Neely III, R. R., Conley, A. J., Vitt, F., and Lamarque, J.-F.: A consistent prescription of
1169 stratospheric aerosol for both radiation and chemistry in the Community Earth System Model
1170 (CESM1), *Geosci. Model Dev.*, 9, 2459-2470, doi:10.5194/gmd-9-2459, 2016.
1171

1172 Poore, R. Z., Quinn, T.M. and Verardo, S.: Century-scale movement of the Atlantic Intertropical
1173 | Convergence Zone linked to solar variability, [Geophys. Res. Lett.](#), 31, L12214, doi:
1174 10.1029/2004GL019940, 2004.
1175

1176 Rasch P. J., Latham, J. and Chen, C.C.: Geoengineering by cloud seeding: influence on sea ice
1177 and climate system, *Environmental Research Letters*, 4, 45-112. doi:10.1088/1748-
1178 9326/4/4/045112, 2009.
1179

1180 | Reason, C. J. C.: Subtropical Indian Ocean SST dipole events and southern African rainfall,
1181 [Geophys. Res. Lett.](#), 28, 2225-2228, 10.1029/2000GL012735, 2001.
1182

1183 Robock, A.: 20 reasons why geoengineering may be a bad idea, *Bull. Atomic Sci.*, 64, 14–18,
1184 doi:10.2968/064002006, 2008.
1185

1186 Robock, A.: Bubble, bubble, toil and trouble. An editorial comment. *Climatic Change*, 105, 383-
1187 385, doi:10.1007/s10584-010-0017-1, 2011.
1188

1189 Robock, A.: Stratospheric aerosol geoengineering, *Issues Env. Sci. Tech.* (special issue
1190 “Geoengineering of the Climate System”), 38, 162-185, 2014.
1191

1192 | [Robock, A.: Albedo enhancement by stratospheric sulfur injection: More research needed.](#)
1193 [Earth’s Future](#), doi:10.1002/2016EF000407, 2016.
1194

1195 Sanderson B.M., O’Neill B., Tebaldi C.: What would it take to achieve the Paris temperature
1196 targets? *Geophys Res Lett*, 1, 10., doi:10.1002/2016GL069563, 2016.
1197

1198 Seitz, R.: Bright water: hydrosols, water conservation and climate change. *Climatic Change*,
1199 105, 365–381, 2010.
1200

1201 Siegenthaler, U., Stocker, T. F., Monnin, E., Luthi, D., Schwander J., Stauffer, B., Raynaud, D.,
1202 Barnola, J. M., Fischer, H., Masson, Delmotte, V., and Jouzel, J.: Stable carbon cycle-climate
1203 relationship during the late Pleistocene, *Science*, 310, 1313–1317, 2005.
1204

1205 Suzuki, R., Behera, S.K., Iizuka, S. and Yamagata, T.: The Indian Ocean subtropical dipole
1206 simulated using a CGCM, *J. Geo. Res.* 109, doi:10.1029/2003JC001974, 2004.
1207

1208 Taylor, K. E., Stouffer, R. J., and Meehl, G. A.: An overview of CMIP5 and the experiment
1209 design, *B. Am. Meteorol. Soc.*, 93, 485–498, doi:10.1175/BAMS-D-11-00094.1, 2012.
1210

1211 Tilmes, S., Fasullo, J., Lamarque, J.-F., Marsh, D. R., Mills, M., Alterskjaer, K., Muri, H.,
1212 Kristjánsson, J. E., Boucher, O., Schulz, M., Cole, J. N. S., Curry, C. L., Jones, A., Haywood,
1213 J., Irvine, P. J., Ji, D., Moore, J. C., Karam, D. B., Kravitz, B., Rasch, P. J., Singh, B., Yoon,
1214 J.-H., Niemeier, U., Schmidt, H., Robock, A., Yang, S., and Watanabe, S.: The hydrological
1215 impact of geoengineering in the Geoengineering Model Intercomparison Project (GeoMIP),
1216 *J. Geophys. Res.-Atmos*, 118, 11036–11058, doi:10.1002/jgrd.50868, 2013.
1217

1218 Tilmes, S., Mills, M. J., Niemeier, U., Schmidt, H., Robock, A., Kravitz, B., Lamarque, J.-F.,
1219 Pitari, G., and English, J. M.: A new Geoengineering Model Intercomparison Project
1220 (GeoMIP) experiment designed for climate and chemistry models, *Geosci. Model Dev.*, 8,
1221 43-49, doi:10.5194/gmd-8-43-2015, 2015.
1222

1223 Tilmes, S., Lamarque, J.-F., Emmons, L. K., Kinnison, D. E., Marsh, D., Garcia, R. R., Smith, A.
1224 K., Neely, R. R., Conley, A., Vitt, F., Val Martin, M., Tanimoto, H., Simpson, I., Blake, D.
1225 R., and Blake, N.: Representation of the Community Earth System Model (CESM1) CAM4-
1226 chem within the Chemistry-Climate Model Initiative (CCMI), *Geosci. Model Dev.*, 9, 1853-
1227 1890, doi:10.5194/gmd-9-1853-2016, 2016.
1228

1229 Trenberth, K. E., and Dai, A.: Effects of Mount Pinatubo volcanic eruption on the hydrological
1230 cycle as an analog of geoengineering, *Geophys. Res. Lett.*, 34, L15702,
1231 doi:10.1029/2007GL030524, 2007.
1232

1233 Wood, R. and Bretherton, C. S.: Boundary layer depth, entrainment, and decoupling in the cloud-
1234 capped subtropical and tropical marine boundary layer, *J. Climate*, 17, 3576–3588, 2004.
1235

1236 Wood, R. and Bretherton, C. S.: On the relationship between stratiform low cloud cover and
1237 lower-tropospheric stability, *J. Climate*, 19, 6425–6432, 2006.
1238

1239 Xia, L., Robock, A., Tilmes, S., and Neely III, R. R.: Stratospheric sulfate geoengineering could
1240 enhance the terrestrial photosynthesis rate, *Atmos. Chem. Phys.*, 16, 1479-1489,
1241 doi:10.5194/acp-16-1479-2016, 2016.
1242

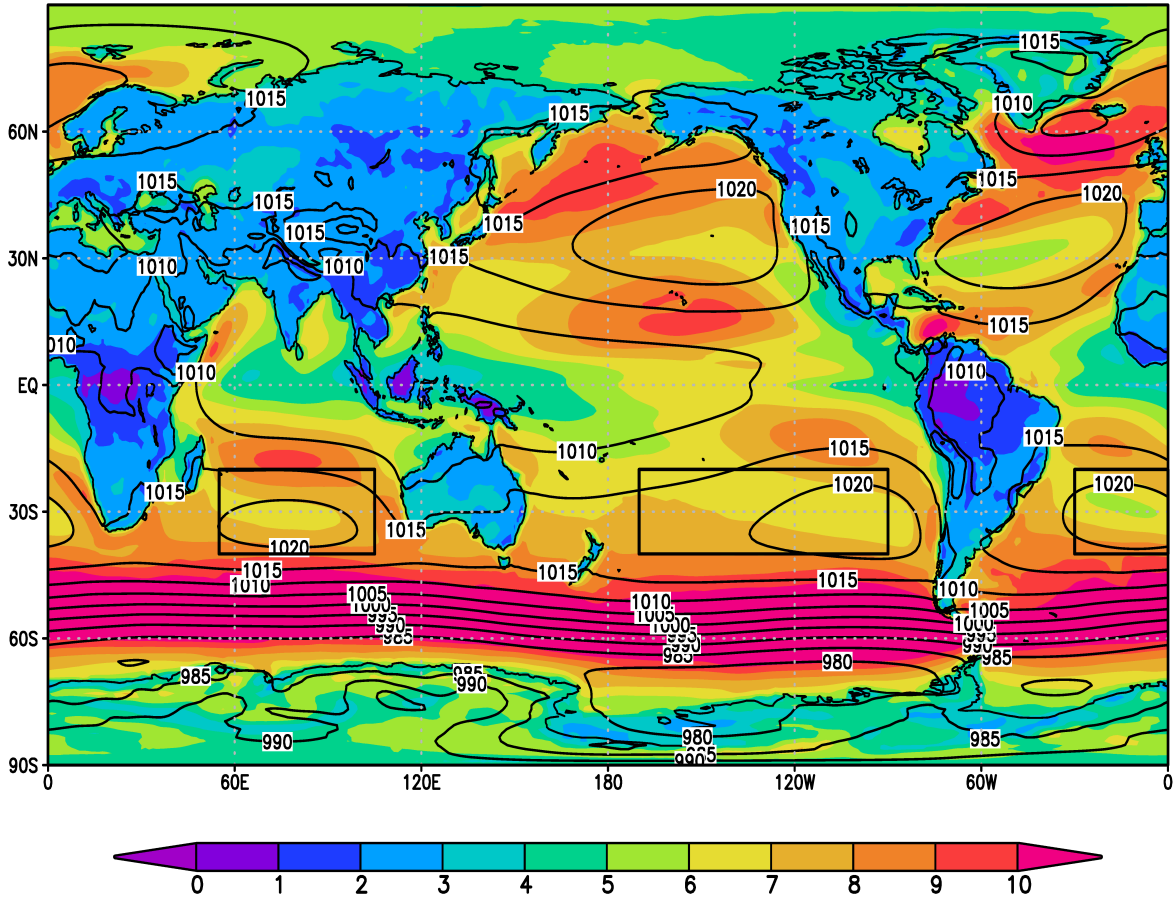
1243 Xie, S-P. and Philander, S. G. H.: A coupled ocean-atmosphere model of relevance to the ITCZ
1244 in the eastern Pacific, *Tellus*, 46A, 340–350, 1994.
1245

1246 **Table 1.** Changes in temperature and precipitation in G4Foam relative to both G4SSA and
 1247 RCP6.0, for the entire globe and for the Tropics (20°S-20°N) annually and in Northern
 1248 Hemisphere summer, for the 40-year period beginning 10 years after the start of climate
 1249 engineering.
 1250

Global, 2030-2069	G4Foam – G4SSA (% change)	G4Foam – RCP6.0 (% change)
Precipitation (mm/day)	+0.02 (+0.61)	-0.06 (-1.98)
Land precipitation (mm/day)	+0.07 (+3.19)	+0.01 (+0.32)
Ocean precipitation (mm/day)	-0.01 (-0.36)	-0.08 (-2.57)
Temperature (K)	+0.27	-0.53
Land temperature (K)	+0.63	-0.44
Global, 2030-2069, June-July-August		
Precipitation (mm/day)	+0.02 (+0.70)	-0.05 (-1.85)
Land precipitation (mm/day)	+0.08 (+3.35)	+0.02 (+0.70)
Ocean precipitation (mm/day)	+0.01 (-0.29)	-0.08 (-2.51)
Temperature (K)	+0.32	-0.60
Land temperature (K)	+0.71	-0.53
Tropical, 2030-2069		
Precipitation (mm/day)	+0.06 (+1.59)	-0.03 (-1.06)
Land precipitation (mm/day)	+0.16 (+3.93)	+0.07 (+1.43)
Ocean precipitation (mm/day)	+0.03 (+0.77)	-0.07 (-1.92)
Temperature (K)	+0.21	-0.60
Land temperature (K)	+0.43	-0.61
Tropical, 2030-2069, June-July-August		
Precipitation (mm/day)	+0.06 (+1.52)	-0.03 (-0.84)
Land precipitation (mm/day)	+0.16 (+4.66)	+0.07 (+2.02)
Ocean precipitation (mm/day)	+0.03 (+0.67)	-0.06 (-1.61)
Temperature (K)	+0.18	-0.61
Land temperature (K)	+0.37	-0.70

1251

CESM-CAM4-CHEM Control 10m wind (m/s)
 shaded, sea level pressure (hPa) contours
 2005-2019. Boxes bound foamed regions.



1252
 1253
 1254
 1255
 1256
 1257
 1258
 1259

Figure 1. Applied forcing and global mean temperature response. Ocean albedo changed from a daily average of 0.06, which includes a very small daily cycle, to a fixed value of 0.15 with no daily cycle, over “foam regions,” 20°N-20°S, 90°W-170°W (South Pacific), 20°N-20°S, 30°W-0°E (South Atlantic) and 20°N-20°S, 55°E-105°E (South Indian). Each foamed region is outlined in black. Control run sea level pressure (mb) is shown with contours and 10-m winds (m/s) are shaded.

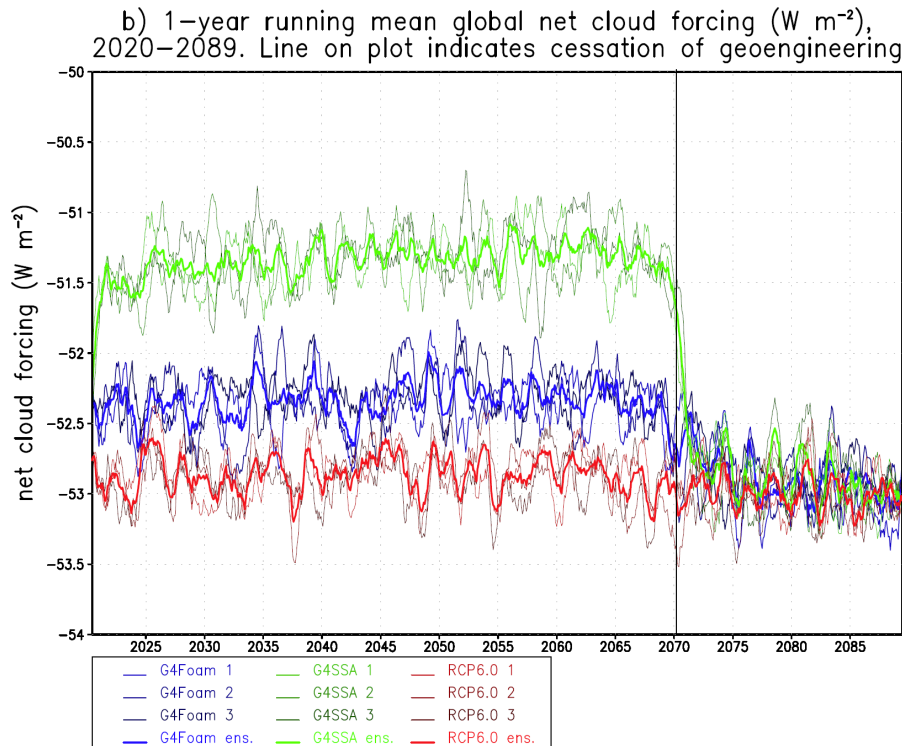
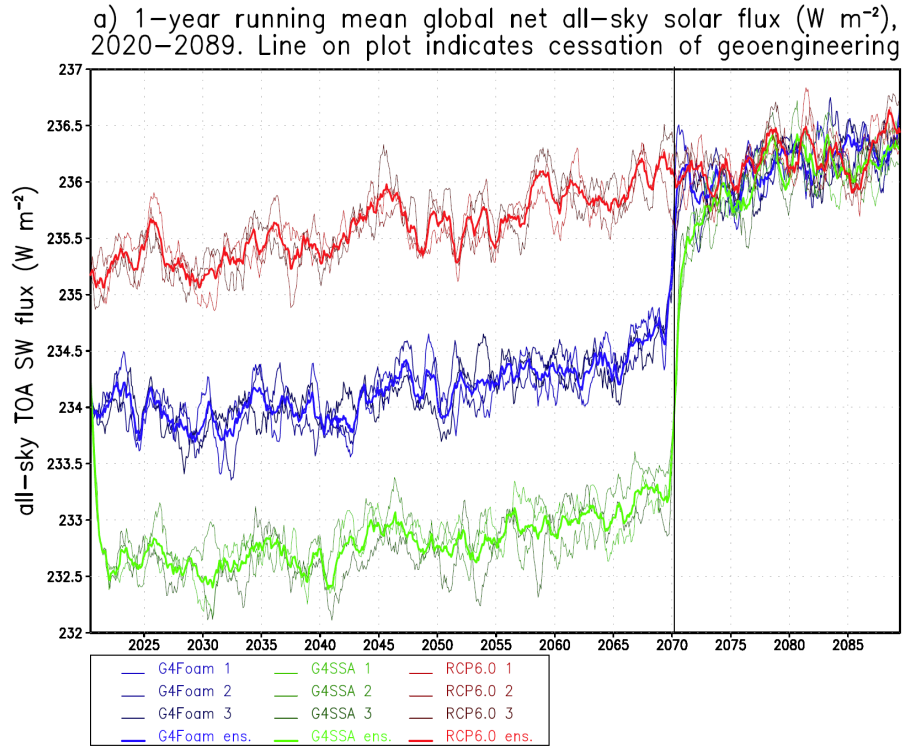


Figure 2. a) Net all-sky SW flux at top-of-atmosphere and (b) Time series of global mean net cloud forcing. Each ensemble member and the ensemble mean are shown for each forcing.

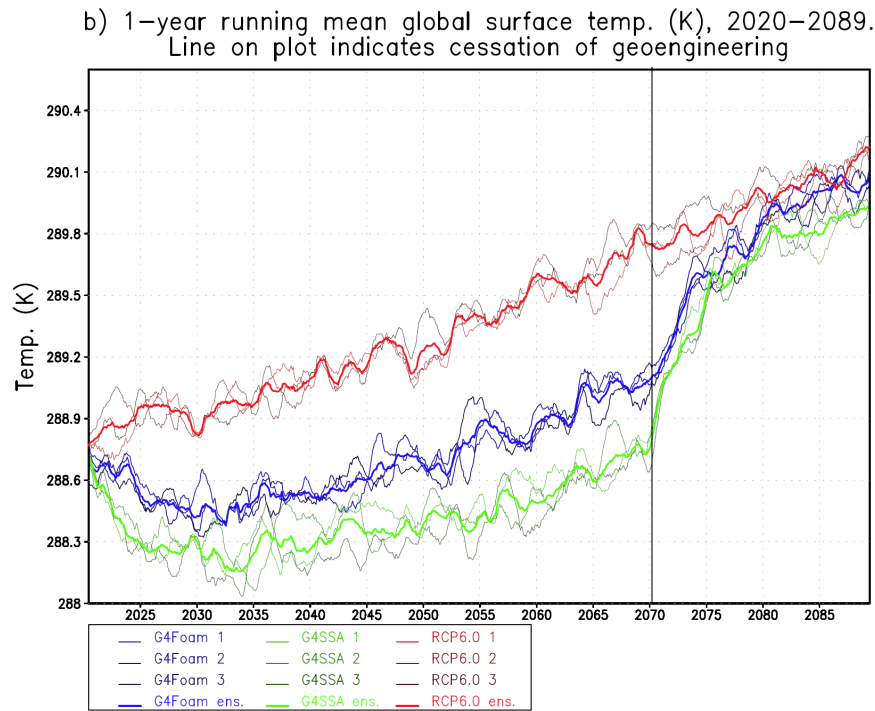
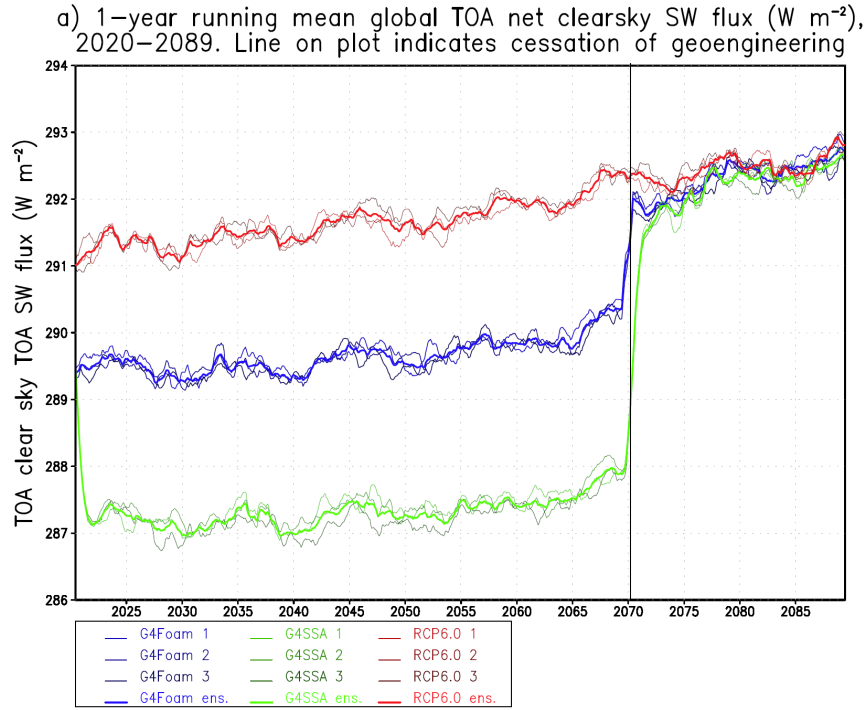
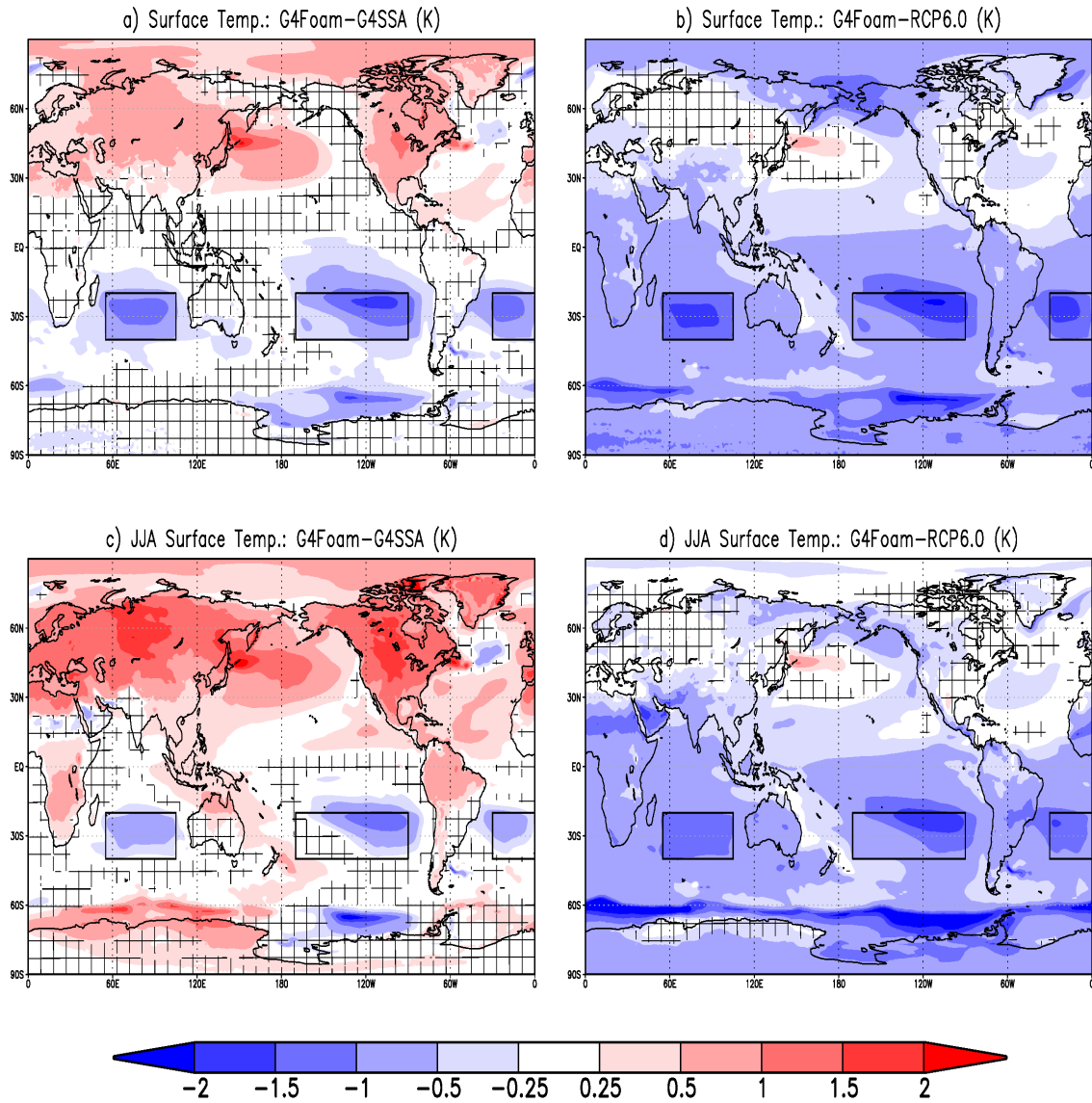
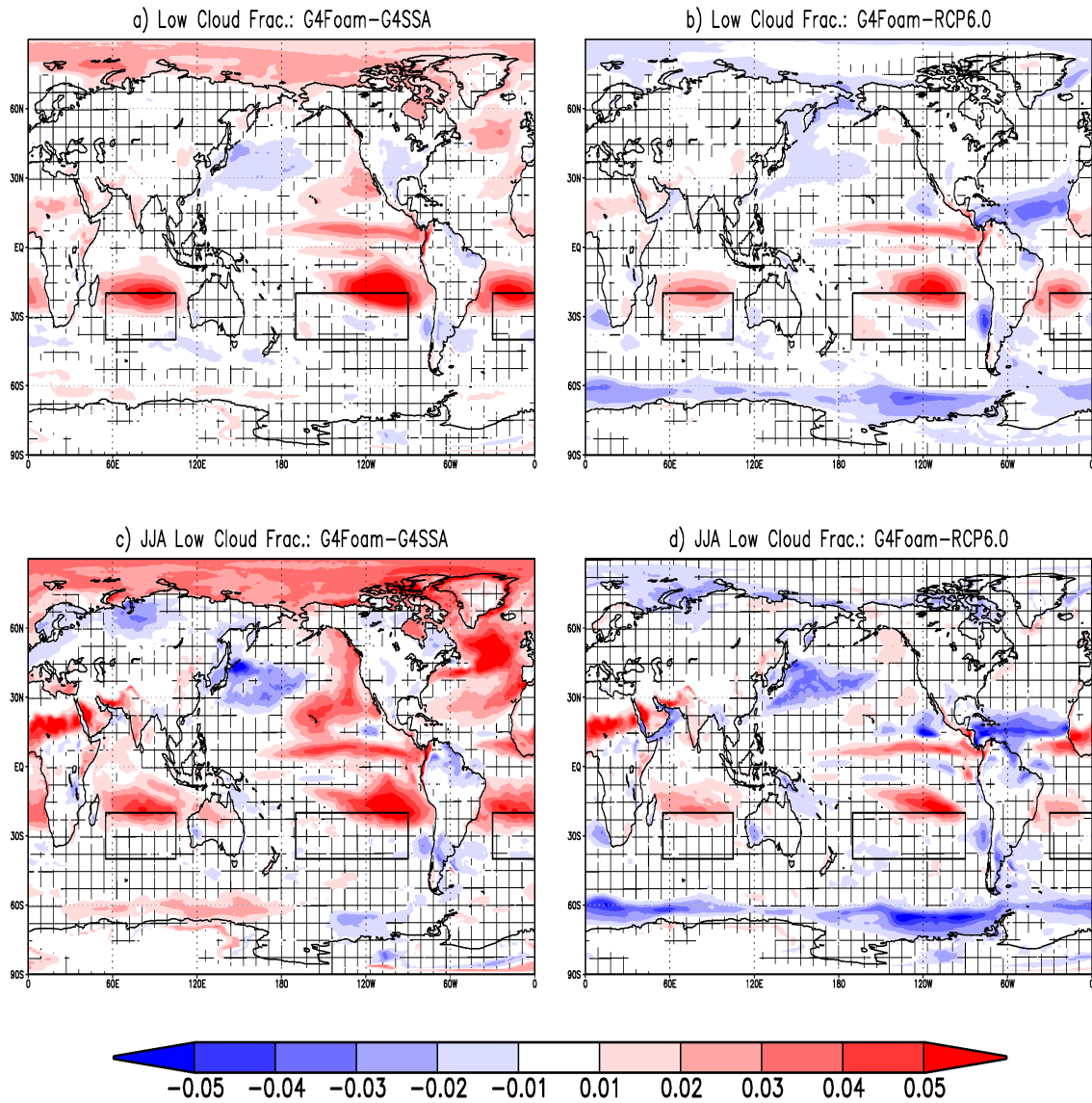


Figure 3. (a) Net clear sky SW flux at top of atmosphere, which includes the effects of changes in radiation caused by changes in ocean surface albedo or land albedo (ice and snow), as well as stratospheric aerosols (stratospheric geoengineering) and (b) Time series of global mean temperature. In G4Foam, temperature is more than twice as sensitive to ocean albedo forcing as it is to stratospheric geoengineering, as applied in G4SSA, albeit with very different latitudinal distributions of temperature changes. Each ensemble member and the ensemble mean are shown for each forcing.



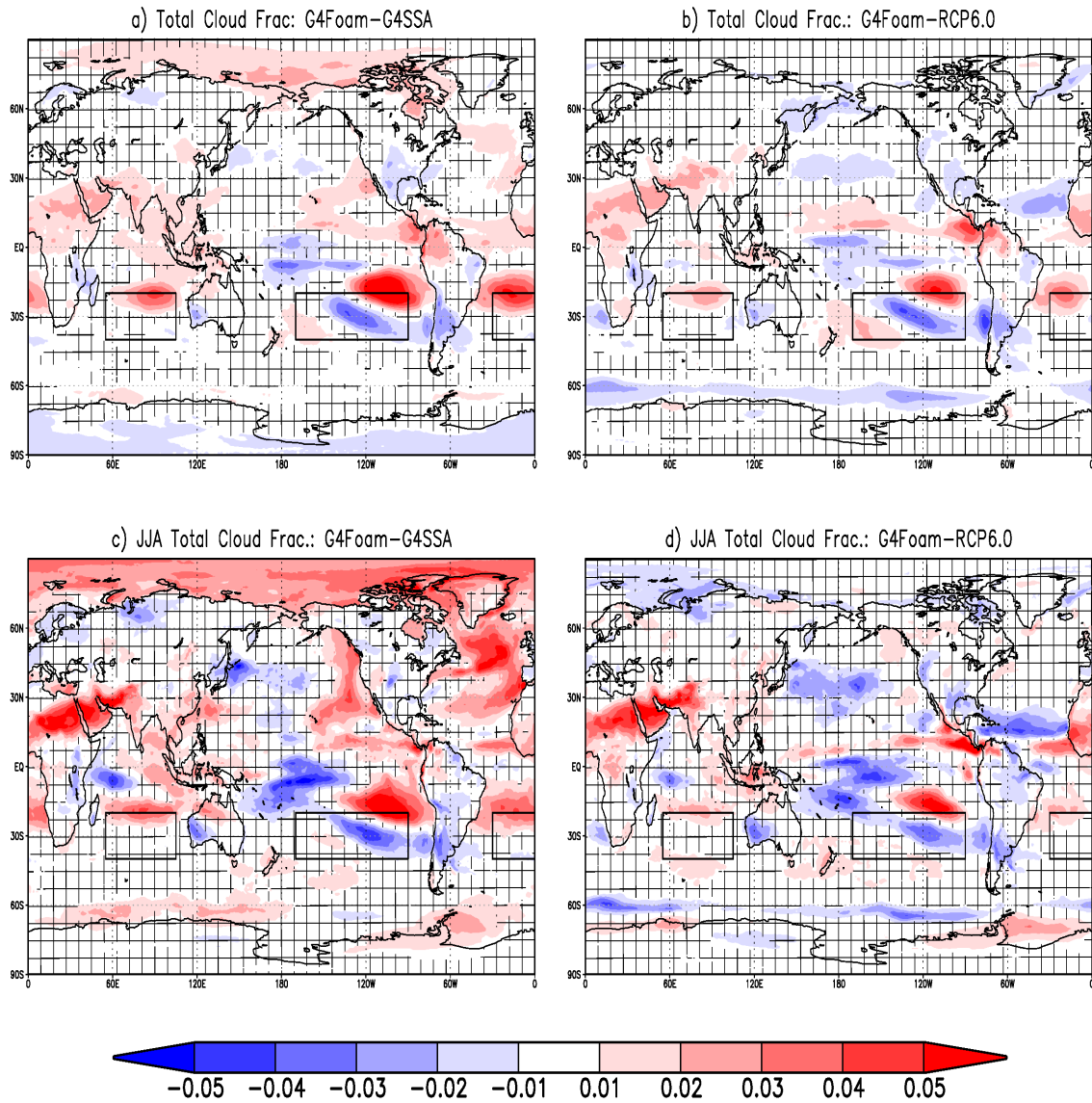
1279
 1280
 1281
 1282
 1283
 1284
 1285

Figure 4. 2030-2069 surface temperature differences (K) between G4Foam and (a) G4SSA, (b) RCP6.0, (c) G4SSA during JJA, and (d) RCP6.0 during JJA. Hatched regions are areas with $p > 0.05$ (where changes are not statistically significant based on a paired t -test). Black boxes enclose foamed regions.



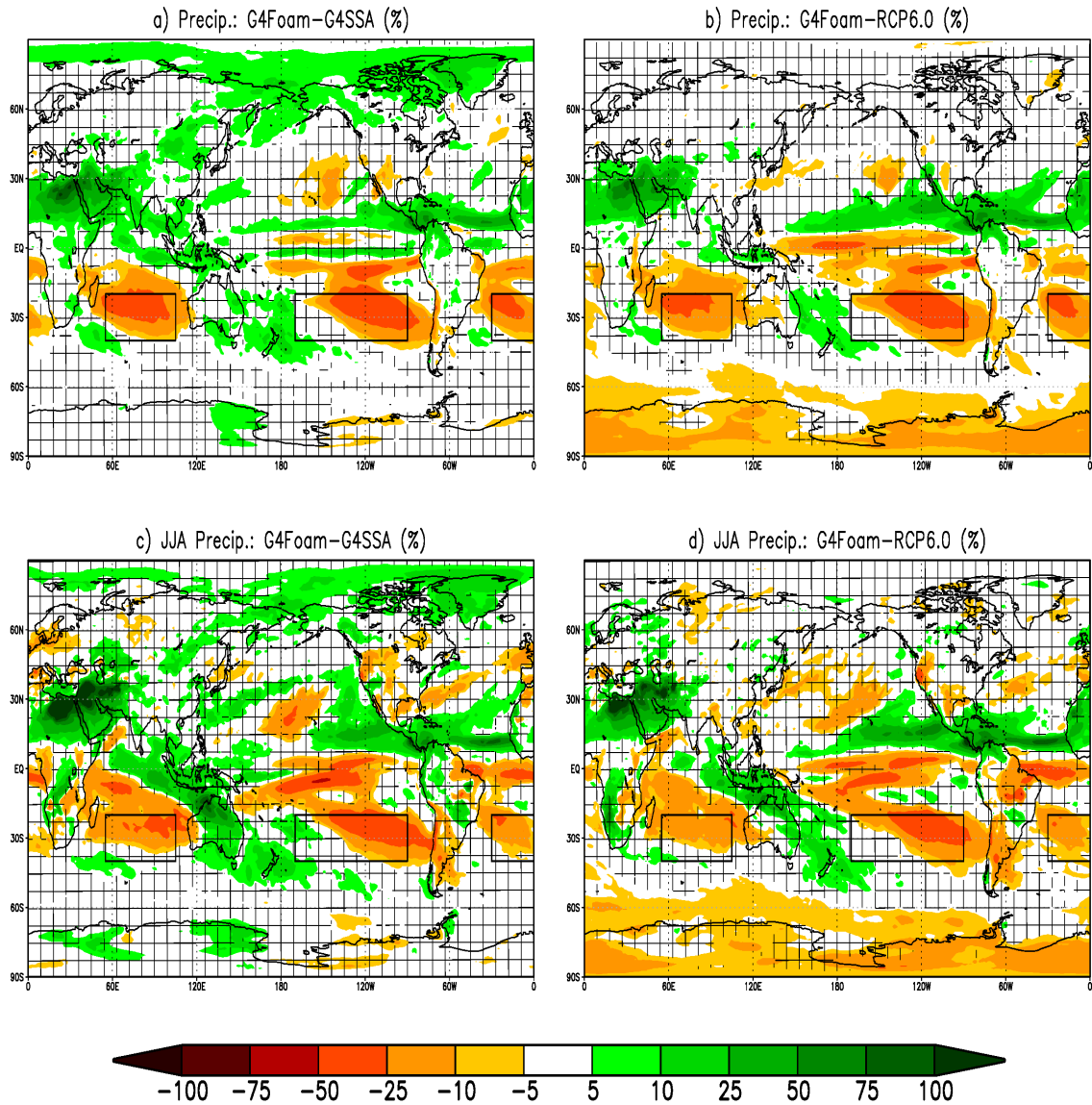
1286
 1287
 1288
 1289
 1290
 1291
 1292
 1293
 1294

Figure 5. 2030-2069 low cloud fraction difference (unitless) between G4Foam and (a) G4SSA, (b) RCP6.0, (c) G4SSA during JJA, and (d) RCP6.0 during JJA. Hatched regions are areas with $p > 0.05$ (where changes are not statistically significant based on a paired t -test). Black boxes enclose foamed regions.



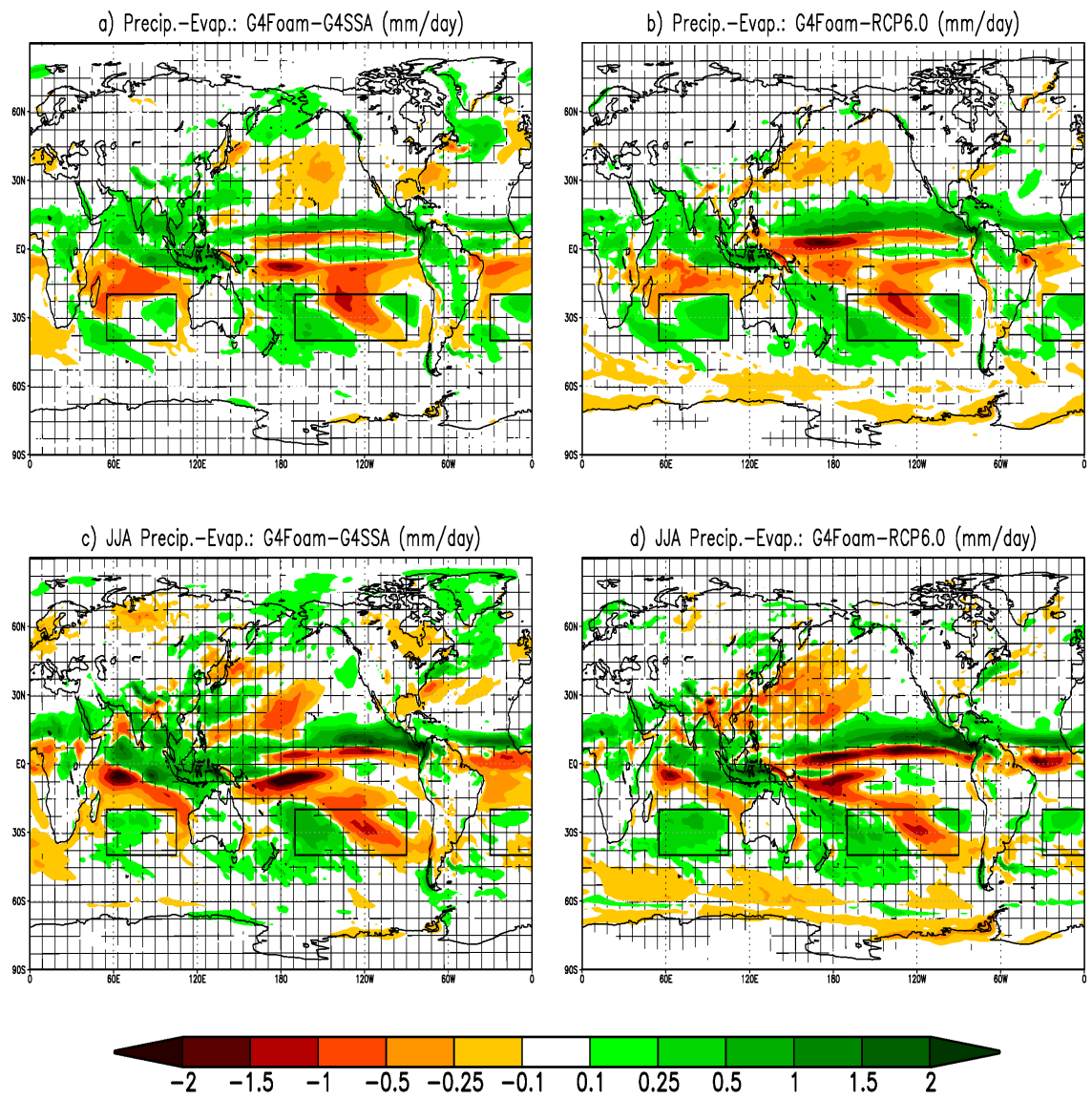
1295
 1296
 1297
 1298
 1299
 1300
 1301
 1302

Figure 6. 2030-2069 total cloud fraction difference (unitless) between G4Foam and (a) G4SSA, (b) RCP6.0, (c) G4SSA during JJA and (d) RCP6.0 during JJA. Hatched regions are areas with $p > 0.05$ (where changes are not statistically significant based on a paired t -test). Black boxes enclose foamed regions.



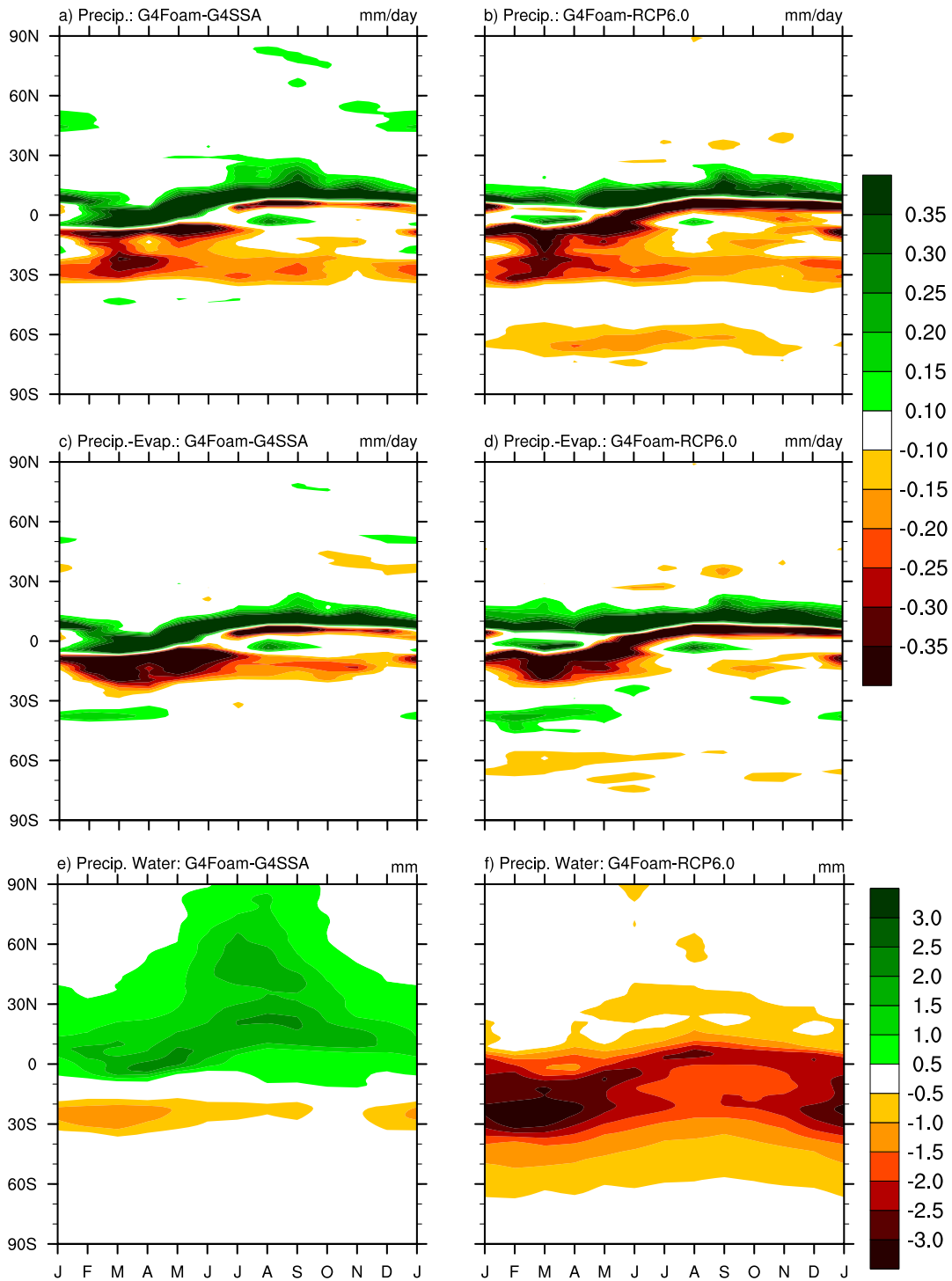
1303
 1304
 1305
 1306
 1307
 1308
 1309
 1310

Figure 7. 2030-2069 precipitation difference (%) between G4Foam and (a) G4SSA, (b) RCP6.0, (c) G4SSA during JJA and (d) RCP6.0 during JJA. Hatched regions are areas with $p > 0.05$ (where changes are not statistically significant based on a paired t -test). Black boxes enclose foamed regions.

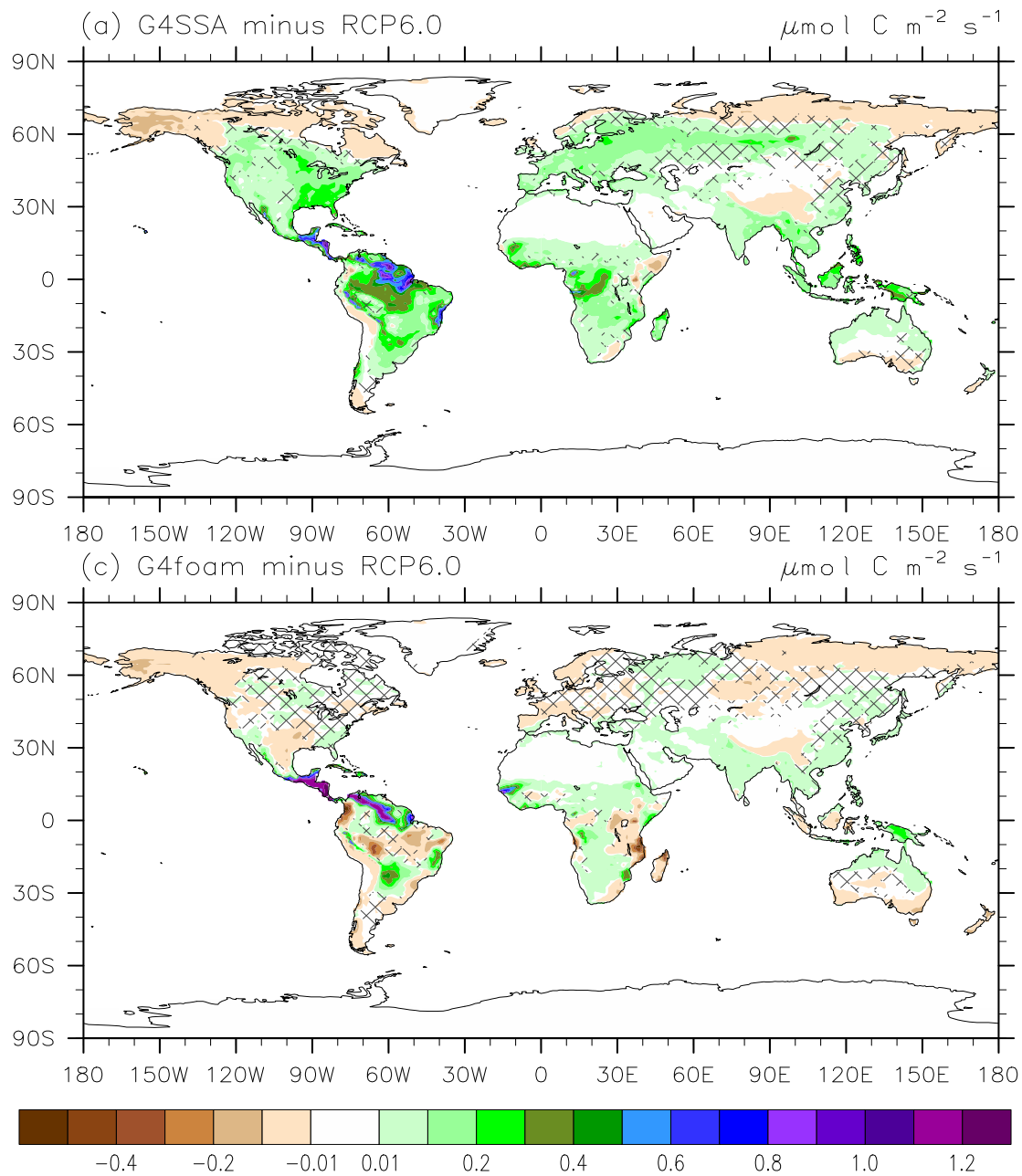


1311
 1312
 1313
 1314
 1315
 1316
 1317

Figure 8. 2030-2069 precipitation minus evaporation difference (mm/day) between G4Foam and (a) G4SSA, (b) RCP6.0, (c) G4SSA during JJA and (d) RCP6.0 during JJA. Hatched regions are areas with $p > 0.05$ (where changes are not statistically significant based on a paired t -test). Black boxes enclose foamed regions.



1318
 1319 **Figure 9.** 2030-2069 monthly mean annual cycle of zonal mean precipitation (mm/day) for (a)
 1320 G4Foam minus G4SSA and (b) G4Foam minus RCP6.0, precipitation minus evaporation
 1321 (mm/day) for (c) G4Foam minus G4SSA and (d) G4Foam minus RCP6.0, and total precipitable
 1322 water (mm) for (e) G4Foam minus G4SSA and (f) G4Foam minus RCP6.0.
 1323



1324
 1325 **Figure 10.** (a) Photosynthesis rate differences between G4SSA and RCP6.0 during years 2030–
 1326 2069 (sulfate injection period, excluding the first 10 years) (Fig. 4a from Xia et al., 2016). (b)
 1327 Photosynthesis rate anomaly between G4Foam and RCP6.0 during years 2030–2069 of solar
 1328 reduction. Hatched regions are areas with $p > 0.05$ (where changes are not statistically
 1329 significant based on a paired t test).